Free Radical Biology and Medicine 224 (2024) 23–38

Contents lists available at ScienceDirect

Free Radical Biology and Medicine

journal homepage: www.elsevier.com/locate/freeradbiomed

Identification of human circulating factors following remote ischemic conditioning (RIC): Potential impact on stroke

Inês G. Mollet [a,b,c,1], Ricardo Viana-Soares [b,1], Catarina Cardoso-Pires [a,c], Nuno L. Soares [b], João Pedro Marto [b,d,e], Marcelo Mendonça [b,f], Cláudia S.F. Queiroga [b], Ana S. Carvalho [b], Catarina O. Sequeira [b,e], Luísa Teixeira-Santos [b,e], Tatiana P. Fernandes [a,c], Kerman Aloria [g], Sofia A. Pereira [b,e], Rune Matthiesen [b], Miguel Viana-Baptista [b,d,e], Helena L.A. Vieira [a,b,c,*]

[a] UCIBIO, Applied Molecular Biosciences Unit, Department of Chemistry, NOVA School of Science and Technology, Universidade Nova de Lisboa, Caparica, Portugal
[b] iNOVA4Health, NOVA Medical School|Faculdade de Ciências Médicas, NMS|FCM, Universidade NOVA de Lisboa, Portugal
[c] Associate Laboratory i4HB, Institute for Health and Bioeconomy, NOVA School of Science and Technology, Universidade NOVA de Lisboa, Caparica, Portugal
[d] Department of Neurology, Hospital de Egas Moniz, Centro Hospitalar Lisboa Ocidental, Portugal
[e] Centro Clínico Académico de Lisboa CCAL, Lisboa, Portugal
[f] Champalimaud Research, Champalimaud Center for the Unknown, Lisbon, Portugal
[g] Proteomics Core Facility-SGIKER, University of the Basque Country UPV/EHU, Vizcaya, Spain

ARTICLE INFO

Keywords:
Remote ischemic (pre)conditioning
Stroke
Proteomics
Biomarkers
Oxidative stress
Neuroinflammation

ABSTRACT

Remote ischemic conditioning (RIC) is a procedure consisting of short cycles of ischemia applied in a limb that activates endogenous protection in distant organs, such as the brain. Despite the promising outcomes of RIC, the biochemical factors governing inter-organ communication remain largely unexplored, particularly in humans. A pilot study on 20 healthy humans was performed to identify potential circulating biochemical factors involved in RIC signalling. Blood was collected before and immediately, 4 and 22 h after the end of RIC. To characterize the responses triggered by RIC, a combination of biochemical and proteomic analysis, along with functional *in vitro* tests in human cells, were performed.

RIC did not alter the levels of nitric oxide, bilirubin and cell-free mitochondrial DNA. In contrast, carboxyhaemoglobin levels increased following RIC at all time points and young subset, suggesting endogenous production of carbon monoxide that is a cytoprotective gasotransmitter. Additionally, the levels of glutathione and cysteinylglycine bound to proteins also increased after RIC, while glutathione catabolism decreased. Plasma proteomic analysis identified overall 828 proteins. Several steps of statistical analysis (Student's t-test, repeated measures ANOVA, with Holm corrected pairwise p-values <0.05 threshold and fold change higher or lower than 100 %) leaded to the identification of 9 proteins with altered circulating levels in response to RIC at 4h and 22h. All 9 proteins are from extracellular space or exosomes, being involved in inflammation, angiogenesis or metabolism control. In addition, RIC-conditioned plasma from young subjects protected microglial cell culture against inflammatory stimuli, indicating an anti-inflammatory effect of RIC. Nevertheless, other functional tests in neurons or endothelial cells had no effect. Overall, we present some evidence for RIC-induced anti-inflammatory and antioxidant responses in healthy human subjects, in particular in young subjects. This study is a first step towards the disclosure of signalling factors involved in RIC-mediated inter-organ communication.

1. Introduction

Preconditioning, conditioning or hormesis is a process that generates cell or tissue protection by stimulating low levels of stress. In fact, biological stress below the damage threshold may activate endogenous mechanisms of defence, producing a state of tolerance and tissue protection. In 1986, it was shown for the first time that short periods (5 min) of heart ischemia induced cardioprotection against longer periods (40

* Corresponding author. UCIBIO, NOVA School of Science and Technology, Universidade NOVA de Lisboa, Campus de Caparica, 2829-526, Caparica, Portugal.
E-mail address: hl.vieira@fct.unl.pt (H.L.A. Vieira).
[1] These authors have equally contributed.

https://doi.org/10.1016/j.freeradbiomed.2024.08.017
Received 21 March 2024; Received in revised form 12 August 2024; Accepted 13 August 2024
Available online 14 August 2024

min) of ischemia [1]. Since then, much research on ischemic preconditioning has been done in different organs, including the brain, using experimental models and some clinical trials [2,3]. Remote ischemic conditioning (RIC) is a variation of ischemic preconditioning in which ischemia (blood flow interruption with a tourniquet) is applied to a non-vital part of the body (for example, an arm) that is distant from the targeted organ to be protected (such as the brain) [4]. RIC presents many advantages: it is a simple, cost-effective and non-invasive technique and the organism is fully adapted to it, presenting almost no side effects [4]. In fact, RIC is a potential therapy based on the endogenous mechanisms of defence that can be used against several diseases, including stroke, dementia, heart attack, among others [3–5].

Stroke is the leading cause of brain disability and the second cause of death worldwide; and it can be haemorrhagic or ischemic [6]. Haemorrhagic stroke corresponds to about 15 % of cases and no specific therapy is available, except lowering blood pressure to limit hematoma. The remaining 85 % of cases are ischemic stroke for which therapies are thrombolysis with recombinant tissue-activated plasminogen (rtPA) or thrombectomy (mechanical removal of thrombi) [7]. Current stroke therapies primarily focus on restoring blood flow (reperfusion), but they do not directly address the repair of damaged brain tissue (brain parenchyma). Consequently, there is a need for the development of novel and effective stroke treatments. RIC emerges as a promising strategy in this effort to find solutions to this unmet medical challenge.

Since its initial application in an experimental model of cerebral ischemia in 2004 [8], neuroscientists have been studying protective effects, cellular and molecular mechanisms of RIC in animal models of stroke. These studies focused on brain tissue processes, namely neural cell death, neuroinflammation, autophagy, neurogenesis, cerebral blood flow or anti-oxidant response [4,9]. Likewise, some potential signalling factors involved in the communication between limb and brain were also identified in experimental models, such as circulating biochemical factors or cells, autonomous nervous system, exosomes or microRNAs [4,10].

More recently, several clinical trials have been performed in ischemic stroke patients during acute phase, with safety, feasibility and tolerability as first outcomes [11–13]. Some clinical trials have revealed promising results of RIC in ischemic stroke patients. Namely, RIC has been associated with a reduction in the National Institute of Health Stroke scale NIHSS score at day 90 post-stroke [14] and it appears to decrease the risk of infarction one month after stroke [11,12]. Furthermore, RIC has been reported to induce changes in circulating biomarkers in acute-phase stroke patients. Specifically, RIC has been associated with increased plasma levels of Heat Shock Protein-27 (HSP-27) [14] and decreased plasma levels of S100β [15].

Nonetheless, no previous human study has been made with the purpose of disclosing the blood signalling molecules affected by RIC in healthy subjects, i.e. no stroke patients. Therefore, our pilot study aims to identify the circulating biomolecular factors that undergo changes in response to arm RIC to contribute to our understanding of how RIC might ultimately confer neuroprotection. For that, twenty healthy volunteers (divided in senior and young subsets) underwent RIC procedure and biochemical and proteomic analysis were conducted in their plasma. Moreover, functional tests of RIC-conditioned plasma were performed in human cell lines of neurons, microglia and endothelial cells from brain microvasculature. The rationale behind this study in healthy volunteers (and not in stroke patients) is to avoid any confounding factors derived from stroke. Thus, any alteration in circulating molecules is attributed to the RIC procedure itself and not to the ischemic disease. Nevertheless, the senior volunteers present age-associated comorbidities, which can influence the RIC response, thus a particular attention was devoted to the data generated from the young subset of volunteers.

2. Material and methods

2.1. Participants

Being a pilot study, a total of 20 subjects were selected according to two age subgroups: senior (>60 years old) and young (<40 years old) between February and September 2017. Senior subjects were recruited from the hospital volunteers association: *Liga dos Amigos HSFX* from *Centro Hospitalar Lisboa Ocidental* (CHLO, Portugal) that is an affiliated Hospital of the *NOVA Medical School* (NMS, Portugal) wherein younger subjects were recruited. The number of subjects for each subgroup concerning age and sex are: 5 for young female and young male, 6 for senior female and 4 for senior male. The study was approved by the NMS Independent Ethical Committee (nº10/2016/CEFCM). The applied exclusion criteria were: any previous neurological disease or neurosurgical procedure, severe heart failure (NYHA class III or higher), peripheral artery disease, skin ulcers or other severe dermatological disease. Subjects were also excluded per investigator judgment if they had any unstable/severe diseases. Informed consent was obtained from all participants before the beginning of the study.

2.2. RIC procedure

The final aim was to characterize changes in proteins and other biochemical molecules following RIC procedure in order to identify potential factors involved in inter-organ RIC signalling and brain tissue protection. The RIC protocol consisted of four cycles of 5-min ischemia/5-min reperfusion, applied to the arm. Ischemia was performed with a blood pressure cuff inflated to above 220 mmHg or at least 20 mmHg above the subject's systolic arterial pressure (Fig. 1A).

2.3. Blood collection

Peripheral blood samples were collected from all participants 1h and 20 min before the beginning of RIC (T0), immediately after RIC (T1) and then 4h (T2) and 22h following end of RIC (T3), which corresponds to 24h after the first blood collection (Fig. 1B). Non-exposure groups (control) correspond to T0, while RIC exposure groups are T1, T2 and T3 for all subjects.

2.4. Haemoglobin and carboxyhaemoglobin quantification

Haemoglobin, namely oxyhaemoglobin, methaemoglobin and carboxyhaemoglobin (COHb) were quantified using AVOXimeter 4000 (A-VOX Systems, Inc., USA). A volume of 40 μL of fresh blood was collected and used for optical quantification. To avoid bias variations, smokers (3 subjects) were excluded from this analysis since their basal levels of COHb are higher.

2.5. Plasma preparation

Blood samples collected in EDTA-coated tubes were centrifuged at 800g for 15 min to obtain plasma. Plasma samples were aliquoted and frozen at −80 °C until further analysis. A pool of 10 plasma samples for each time point from young subjects were prepared for functional validation in human cell culture.

2.6. Plasma analysis

2.6.1. Bilirubin quantification

The Bilirubin assay kit (Sigma-Aldrich, MAK-126) was used following the kit protocol. The kit follows Jendrassik-Grof method for the quantification of bilirubin, which is based on the reaction of bilirubin with diazotized sulfanilic acid, resulting in a colorimetric product measured at 530 nm.

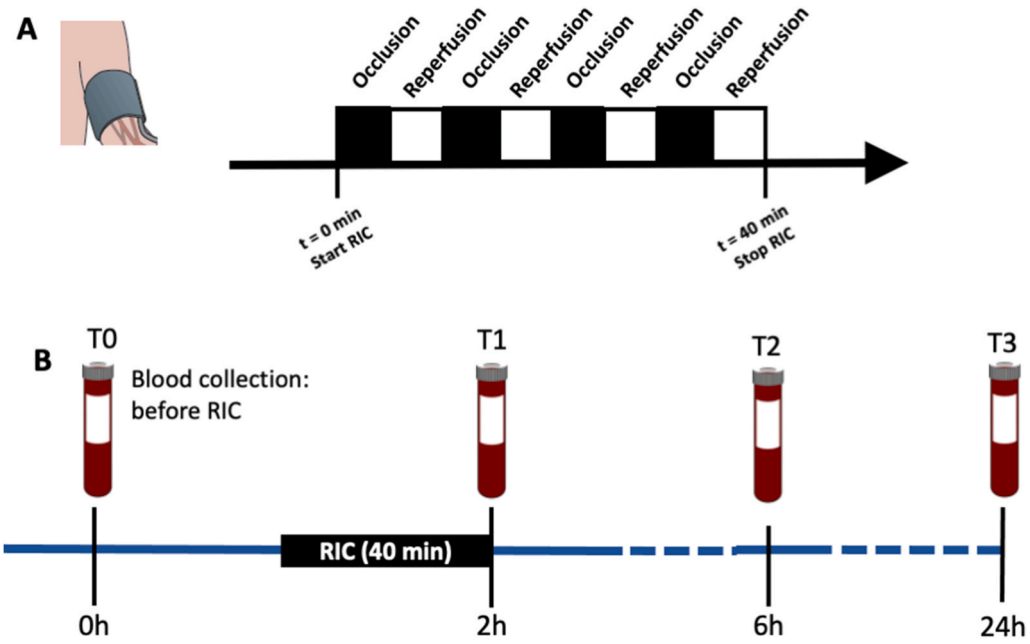

Fig. 1. Remote ischemic conditioning (RIC) procedure. (A) RIC procedure in the arm and time-course of RIC procedure (time in minutes). Four periods of 5 min occlusion were applied with an inflated limb-cuff, each period followed by 5 min of rest (cuff deflated). **(B)** Timeline of blood collection: blood was collected from young and senior volunteers 1h40 min before end of RIC procedure (T0), immediately after RIC (T1), 4h (T2) and 22h after RIC (T3) corresponding to one day after the first blood collection.

2.6.2. Nitric oxide quantification – griess reaction assay

The levels of nitrite, an indicator of the inflammatory marker nitric oxide (NO), were measured by Griess reaction colorimetric test. Plasma was incubated with Griess reagent (1:1 ratio, ref. 0355, Sigma-Aldrich) for 10 min at room temperature, protected from light. Absorbance was measured at 540 nm using an Infinite F200 PRO microplate reader (Tecan). Nitrite concentration was calculated with reference to a standard curve generated from known concentrations of sodium nitrite ($NaNO_2$, Sigma-Aldrich).

2.6.3. Mitochondrial DNA quantification

Genomic DNA was extracted from plasma using the High Pure PCR Template preparation kit (Roche Diagnostics, Mannheim, Germany). PCR was performed using specific forward and reverse primers designed for the mitochondrial COXII gene (5′-ACAGACGAGGTCAACGATCC-3′ and 5′-AGATTAGTCCGCCGTAGTCG-3′) and for the nuclear GAPDH gene (5′-GCATCCTGGGCTACACTGAG-3′ and 5′-GTCAAAGGTGGAG-GAGTGGG-3′), respectively. GAPDH gene was used as reference for mitochondrial DNA quantification. Fast Start DNA Master Plus SYBR Green I (Roche Diagnostics) was used with the experimental run protocol: denaturation program was 95 °C for 10 min, followed by 45 cycles of 95 °C for 15″, 60 °C for 6″ and 72 °C for 20''.

2.6.4. Assessment of glutathiomic profile by high performance liquid chromatography (HPLC)

An HPLC with fluorescence detection was used to quantify the *glutathiomic* profile, namely glutathione (GSH) and other related thiol metabolites (glutathiolomic profile), including cysteinylglycine (CysGly), which is a product of GSH degradation; cysteine (Cys), which is a precursor of GSH synthesis, and homocysteine (HCys), which is a precursor of Cys. Moreover, these molecules were quantified for their total amount, their free and bound to proteins forms. Due to technical and time limitations the number of analysed subjects were: 8 for young and senior subgroups, 5 for male subgroup and 11 for female subgroup.

Aminothiols in plasma were reduced with tris(2-carboxyethyl) phosphine (TCEP) and derivatized with ammonium 7- fluoro-2,1,3-benzoxadiazole-4-sulfonate (SBD-F), as previously described by our group [16]. Samples were analysed by HPLC system (Shimadzu) with a RF-10AXL fluorescence detector, operating at 385 nm (λ excitation) and 515 nm (λ emission). The analytes Cys, HCys, CysGly and GSH were separated on a LiChrospher 100 RP-18 (250 × 4 mm, 5 μm; Merck), with a mobile phase consisting of a mixture of 0.1 M acetate buffer (pH 4.5, adjusted with acetic acid): methanol (99:1 v/v), at a flow rate of 0.8 mL/min, at 29 °C. The run time was 20 min.

2.6.5. Preparation of plasma for proteomics MS analysis

The 14 most abundant proteins of plasma were eliminated using a commercially available kit (Agilent Human 14 Multiple Affinity Removal System Spin Cartridges for the High-Abundant Proteins from Human Proteomic Samples) following procedure instructions. Then, samples were further treated for protein digestion. Protein solution containing SDS and DTT were loaded onto filtering columns and washed exhaustively with 8 M urea in HEPES buffer [17]. Proteins were reduced with DTT and alkylated with IAA. Protein digestion was performed by overnight digestion with trypsin sequencing grade (Promega).

2.6.6. Mass spectrometry analysis

Mass spectrometry analysis was performed by nano LC-MS/MS using a Q-Exactive (Thermo, San Jose, CA) mass spectrometer coupled to an EASY-nLC 100 liquid chromatography system (Thermo, San Jose, CA) via a Nanospray Flex Ion Source. Peptides were loaded onto an Acclaim PepMap100 pre-column (75 μm × 2 cm, Thermo, San Jose, CA) connected to an Acclaim PepMap RSLC (50 μm × 15 cm, Thermo, San Jose, CA) analytical column. Peptides were eluted from the column using a linear gradient of 3–30 % acetonitrile in 0.1 % formic acid at a flow rate of 300 nL/min over 190–254 min LC gradient (120 min for the peptide pull-down). The mass spectrometer was operated in positive ion mode. Full MS scans were acquired from *m/z* 350 to 2000 (1850 for peptide pull-down data) with a resolution of 70.000 at m/z 200. The ten most intense ions were fragmented by higher energy C-trap dissociation with normalized collision energy of 28 and MS/MS spectra were recorded with a resolution of 17.500 at m/z 200. The maximum ion injection time was 120 min for both survey and MS/MS scans, whereas AGC target values of 3×10^6 and 5×10^5 were used for survey and MS/MS scans,

respectively. To prevent repeated sequencing of peptides, dynamic exclusion was applied for 30 s. Singly charged ions or ions with unassigned charge state were also excluded from MS/MS. Data were acquired using Xcalibur software (Thermo, San Jose, CA).

2.6.7. Proteomics annotation

The obtained data from the 124 LC-MS runs were searched using VEMS [18,19]. A standard human proteome database from UniProt (3AUP000005640). Permutated protein sequences, where Arg and Lys were not permutated, were included in the database. Trypsin cleavage allowing a maximum of 4 missed cleavages was used. Carbamidomethyl cysteine was included as fixed modification. Methionine oxidation, N-terminal protein acetylation and lysine acetylation was included as variable modifications. 5 ppm mass accuracy was specified for precursor ions and 0.01 *m/z* for fragment ions. The false discovery rate (FDR) for protein identification was set to 1 % for peptide and protein identifications. No restriction was applied for minimal peptide length for VEMS search. Identified proteins were divided into evidence groups as defined by Matthiesen and co-authors [19].

2.6.8. In silico functional analysis of proteomics data and fold changes

Proteomics data was normalized to total ion counts (iBAQ) per sample, to reduce biases resulting from sample handling and instrumentation. For protein level analysis, Log2(norm+1) was used in pairwise comparisons between time points T0 versus T2 and T3, where "norm" is the normalized ion counts (median ions counts per sample were 1.67×10^{10}. In order to obtain normally distributed data, iBAQ ion counts were Log2 transformed after adding +1 count to all iBAQ values, to eliminate Log of zero error when no signal is detected. Statistical significance was evaluated using two-tailed paired two-sample equal variance Student's t-test and repeated measures ANOVA, with 0.05 threshold chosen for statistical significance; Benjamini-Hochberg and Holm methods were used to correct for multiple testing. R code [R version 4.3.2 (2023-10-31), https://www.r-project.org/] was used to create volcano plots and perform repeated measures ANOVA and violin plots (R code and data used is in Supplementary File 1). p-values indicated by #<0.1, * <0.05, ** <0.01, *** <0.001. Functional analysis of proteins was performed using DAVID Bioinformatics Resources 6.8 [20,21] with Gene annotation derived from GENERIF summaries [22] and Gene Ontology [23,24].

2.7. Functional plasma tests

Control and RIC-derived plasma were always supplemented at a final concentration of 5 % in the cell culture medium for functional cellular evaluation. Because serum (FBS) and plasma are very important in supplementing growth factors and other cytoprotective factors, all cell culture conditions must present the same concentration of (FBS) serum/plasma composition. Thus 5 % of FBS was exchanged for 5 % of human plasma. With this strategy we can assure that any beneficial effect of plasma is due to plasma itself and not to an increase on serum/plasma supplementation, avoiding any confounding effects.

2.7.1. SH-SY5Y human neuroblastoma cell line: maintenance and differentiation

SH-SY5Y human neuroblastoma cell line was purchased from ATCC (American Type Culture Collection). Maintenance of undifferentiated cells: SH-SY5Y cell line was cultured in DMEM/F-12 supplemented with 10 % (v/v) foetal bovine serum (FBS) and 2 % (v/v) Pen/Strep (growth medium). Cells were maintained in a humidified atmosphere of 5 % (v/v) CO_2 at 37 °C. Undifferentiated cells were grown in 75 cm^2 T-flasks and sub-cultured with fresh growth medium, whenever cell confluence was achieved (about 80–90 % cell confluence). Cells were detached by trypsinization at room temperature and slight shaking and hitting to drain down cells with trypsin and resuspended in growth medium in a 1:4 cell passage. Growth medium was changed twice a week. For neuronal differentiation and cell treatment protocols, cells were plated on 24 well plates at 5×10^4 cell/well, following trypsinization and resuspension in growth medium. Neuronal differentiation was induced 24 h after plating undifferentiated cells to ensure attachment and cell differentiation. Neuronal differentiation was stimulated using DMEM/F-12 medium, reduced serum to 1 % (v/v) FBS, 2 % (v/v) Pen/Strep and supplemented with 10 μM of *all-trans* RA (differentiation medium). Differentiation medium was replaced twice (day 1 and day 4) during 6 days of treatment. Of note, SH-SY5Y differentiated neuronal cells present neuronal specific proteins and synaptic markers such as synaptophysin [25].

2.7.2. Plasma treatment of differentiated SH-SY5Y cell line

After differentiation process (at day 6), culture medium was replaced with new medium in 5 experimental conditions: the control condition with 6 % FBS; the pre-RIC condition using 1 % FBS plus 5 % human plasma (T0); and three post-RIC conditions using 1 % FBS plus 5 % conditioned human plasma from T1, T2 and T3, respectively. These supplementations allow the maintenance of final 6 % of serum (FBS)/plasma in all conditions.

2.7.2.1. Flow cytometry for cell viability assessment. SH-SY5Y cells were treated with 1 % FBS +5 % conditioned human plasma at the study time points: T0 to T3 for 24h, followed by cell death induction with *t*-BHP (*tert*-Butyl hydroperoxide) at concentrations ranging from 0 to 32 μM for 18 h. Cells were collected by trypsinization and stained with dye propidium iodide (PI, Invitrogen) at 1 g/mL. Cells were gated by forward and side scatter. A flow cytometer (Attune NxT Acoustic Focusing) was used to analyse cell death-associated parameters. Data analysis was performed using FlowJo® software (10.5.3).

2.7.3. Microglial cell culture

Human HMC3 microglial cell line was purchased from ATCC (American Type Culture Collection). For the maintenance of HMC3 cell line, cells were kept in Minimum Essential Media (MEM) supplemented with 11 % (v/v) non-inactivated Foetal Bovine Serum (FBS) and 1 % (v/v) Penicillin/Streptomycin (Pen/Strep) (Sigma and Gibco Life Technologies, respectively). Cells were maintained in 75 cm^2 T-flasks (Corning) and 25 cm^2 T-flasks (Corning), while passages were performed once to two times a week in 1/2 dilution, depending on cell confluency. BV2 murine microglia cell line (ICLC, Genova, Italy) was cultured in RPMI-1640 (Biowest) supplemented with 10 % (v/v) non-inactivated Foetal Bovine Serum (FBS) and 1 % (v/v) Penicillin/Streptomycin (Pen/Strep) (Sigma and Gibco Life Technologies, respectively). Cells were maintained in 75 cm^2 T-flasks (Corning), while passages were performed two to three times a week in 1/4 dilution, depending on cell confluency.

2.7.4. Plasma treatment of microglial HMC3 cells and inflammation stimulation

HMC3 cells were plated onto 96-well plates according to an optimized seeding of 8.5×10^3 cells/well. After 48 h, medium of HMC3 cell culture was exchanged for media containing: the control condition with 11 % FBS, the pre-RIC condition using 6 % FBS plus 5 % human plasma T0, and three post-RIC conditions using 6 % FBS plus 5 % conditioned human plasma T1, T2 and T3, respectively. After 24 h, inflammation was stimulated with 500 ng/mL LPS (Sigma) for 24h, then ATP at 5 mM (Sigma) was also added; and 30 min later cells were analysed. The composition of serum/plasma supplementation follows the same previous rationale: the maintenance of same final 11 % of serum/plasma in culture media for all conditions.

2.7.5. Plasma treatment of microglial BV-2 cells and inflammation stimulation

BV-2 cells were plated onto 24-well plates, after 24h RIC-conditioned

plasma at 5 % was added into the culture, and 24h later 0.5 μg/mL of lipopolysaccharide (LPS) was added to promote neuroinflammation. The levels of nitrite, an indicator of the inflammatory marker NO, were measured using the culture medium by Griess assay (0355, Sigma) according to Ref. [26].

2.7.6. Measurement of Reactive Oxygen Species generation

Reactive Oxygen Species (ROS) generation was followed by the conversion of 2′,7′-dichlorofluorescein diacetate (H_2DCFDA, Invitrogen, UK) to fluorescent 2′, 7′-dichlorofluorescein (DCF) [27]. After HMC3 treatments, supernatant was removed and cells were incubated for 20 min with 5 μM of H_2DCFDA prepared in PBS. Cells were washed twice, and fluorescence was measured (λ_{exc}: 485 nm, λ_{em}: 530 nm) using Tecan Infinite F200 Pro microplate reader.

2.7.7. Brain microvasculature endothelial cells hCMEC D3 cell culture

The hCMEC/D3 cell line was kindly supplied by Dr Couraud (INSERM, Université René Descartes, Paris, France) [28]. Cells were grown in EBM-2 medium supplemented with VEGF, IGF-1, EGF, basic FGF and hydrocortisone as recommended by the manufacturer, 2.5 % FBS and 1 % (v/v) of Penicillin/Streptomycin (Gibco). The cell medium was changed every 48 h, and the cells reached confluence after 5–6 days of culture. All the cell lines were kept in a humified incubator at 37 °C and 5 % CO_2. hCMEC D3 cerebral endothelial cells were differentiated for 11 days in microwell inserts using 12 well plates using differentiating medium (EBM-2 medium supplemented with Hepes, basic FGF, hydrocortisone, 1 % of Pen/Strep and 2.5 % of FBS as recommended by the manufacturer).

2.7.8. Lucifer yellow permeabilization assay for hCMEC D3 cell line

Differentiated hCMEC D3 cells were treated in 4 experimental conditions: the control condition with 5 % FBS, the pre-RIC condition using 5 % human plasma T0, and two post-RIC conditions using 5 % conditioned human plasma T2 and T3, respectively. Then Lucifer yellow (LY) (L0144, Sigma) was added at the apical side for a final concentration of 20 μM, following 45 min, 25 μL of culture medium from basolateral compartment were collected for fluorescence quantification (λEx = 485 nm and λEm = 535 nm) using Tecan Infinite F200 Pro microplate reader. Permeability coefficient was calculated based on the formula:

$P_{app} = (V_A/A \text{ x time X})/((\text{LY basolateral concentration at time X})/(\text{LY apical concentration at time zero})$, where VA is basolateral volume, A is insert area and time X is 45 min.

2.7.9. Immunofluorescence microscopy for beta-tubulin III assessment

SH-SY5Y cells were fixed with 4 % (v/v) PFA for 20 min at room temperature, and then permeabilized with 0.3 % Triton X100 in PBS for 15 min. After permeabilization, cells were blocked with BlockPerm (0.1 % Triton X100, 1 % BSA in PBS) for 30 min at room temperature. The cells were washed with PBS and incubated in a humified box at RT with the primary antibodies, mouse anti-β tubuline III (Merk Millipore MAB #1637) diluted 1/500 in BlockPerm for 2 h. After washing with PBS, cells were labelled for 1 h with fluorescent secondary antibody, goat anti-mouse conjugated to Alexa Fluor 488 (Thermofisher) diluted January 2000. Coverslips were washed with PBS and mounted onto glass slides with Prolong mounting media (with DAPI - Invitrogen). Fluorescence imaging was done using a Zeiss AxioImager D2 fluorescence microscope.

2.7.10. Western blots for quantification of α-Synaptophysin

Differentiated SH-SY5Y cells were lysed using RIPA buffer and their extracts were separated under reducing electrophoresis on a 1 mm 15 % sodium dodecyl sulfate-polyacrylamide (SDS-PAGE) gel, for 1 h under 150V. Samples were transferred to a nitrocellulose membrane (HybondTMC extra, Amersham Biosciences) for 1 h under 500 mA. Synaptophysin and Actin proteins were stained with α-Synaptophysin (Thermofisher, SY38) or β-actin (Sigma-Aldrich, A5441) antibodies at 1/5000 dilution for 2 h at room temperature.

Blots were developed using the ECL (enhanced chemiluminescence) detection system after incubation with HRP-labelled anti-mouse IgG anti-body (Amersham Biosciences Bioscience), 1/5000, 1 h of incubation at room temperature.

2.8. Statistical analysis

In the proteomic analysis, only the proteins detected in at least half of the samples in each group in at least one of the time points were used for downstream analysis. iBAQ values were normalized to total ion count per sample and Log2 transformed to normalize data distribution, before statistical analysis with R statistical software. Volcano plots were used to visualize overall data significance. Significance was determined by paired Student's t-tests between time points with p-values corrected for multiple protein comparisons using Benjamini-Hochberg procedure. Repeated measures one way-ANOVA was used to analyse data across time points before and after RIC with Holm corrected pairwise p-values determined between time points. R code is provided in Supplementary File 1. Functional analysis and annotation of proteins was performed with the Database for Annotation, Visualization and Integrated Discovery (DAVID) Bioinformatics Resources [Huang 2009 (https://doi.org/10.1038/nprot.2008.211); Sherman 2022 (doi:10.1093/nar/gkac194]).

Reported data on biochemical and functional analysis were statistically evaluated using GraphPad Prism 9. Statistical analysis was performed using two-sample Student's t-test with paired or unpaired samples, or two-way ANOVA. Results concerning the functional analysis of RIC-derived plasma on human cell cultures correspond to at least 3 independent experiments. The used test and the number of replicas are indicated in the figure legends.

Multivariate analyses were performed to assess differences in the panel of biochemical parameters among volunteers. The dataset consisted of 18 biochemical parameters (NO, carboxyhemoglobin, bilirubin and mtDNA and total, free total and protein-bound forms of Cys, CysGly, HCys and GSH) x 64 observations. Data were mean-centered and scaled to unit variance before statistical analysis. Partial Least Square Discriminant Analysis (PLS-DA) was performed to disclose the most relevant biochemical parameters discriminating Young and Senior subgroups, as well as Male and Female subgroups. The parameters with a variable importance on the projection (VIP) value > 1.6 were selected as the most relevant. Principal Component Analysis (PCA) and PLS-DA were performed with SIMCA software, version 14.1 (MKS Umetrics, Umeå, Sweden).

3. Results

3.1. Subjects

RIC was applied to the arm with 4 cycles of 5 min of ischemia and 5 min of reperfusion, with procedure completed in 40 min (Fig. 1). Twenty volunteers separated into two distinct subgroups of 10 volunteers according to age were tested. The age average was 28.9 ± 6.3 years old for young subgroup and 69.1 ± 7.4 years old for Senior subgroup. For detailed information on sex and vascular risk factors see Supplementary Table 1.

3.2. Changes in biochemical factors in plasma following RIC procedure

Biochemical markers were measured to unveil the factors influencing inter-organ communication associated to RIC in healthy volunteers. Additionally, data was analysed for the Young and for Senior groups separately to evaluate potential variations in stress response associated

with aging.

Haem-oxygenase-1 (HO-1) cleaves haem group into carbon monoxide (CO), free Fe2+ and bilirubin and its expression increases in response to stress [29]. CO and bilirubin cytoprotective and anti-inflammatory in several tissues, including the brain [29]; thus, their levels were measured in circulation before and after RIC procedure. CO was indirectly evaluated by the quantification of carboxy haemoglobin (COHb) in the blood (Fig. 2A). COHb levels increased following RIC, suggesting a potential induction of HO-1 in response to the mild stress prompted by RIC. Likewise, increase in COHb levels were observed in Young subsets (Supplementary Fig. 1A), while no difference was found between female and male subgroups (Supplementary Fig. 1B).

Plasma bilirubin levels remained unchanged in response to RIC (Fig. 2B). Although no alterations were found between Young and Senior subgroups (Supplementary Fig. 1C), there is a trend of higher bilirubin circulating levels in senior subjects, which is in accordance with an increase on bilirubin levels during aging [30]. In addition, the levels of bilirubin are higher in male subgroup (Supplementary Fig. 1D). Because both CO and bilirubin are products of HO-1 activity, it would be expectable to detect an increase in both molecules in the plasma, but it did not occur. Nevertheless, alteration in bilirubin plasma levels must be high in order to be detected, being originated in the liver. Moreover, CO levels increased only slightly and were detected as COHb since CO rapidly binds to haemoglobin in circulation. Thus, one can speculate that the small increased levels of CO (measured via COHb with an accurate device) may be locally generated (endothelial cells) at the vessels nearby RIC application. In fact, mechanical pressure of RIC procedure along with ischemic insult may indeed upregulate HO-1 in endothelial cells, increasing its activity.

Nitric oxide (NO) is another key gasotransmitter involved in vasomodulation (generated by endothelial nitric oxide synthase - eNOS), inflammatory response (generated by inducible nitric oxide synthase - iNOS) and preconditioning response [31]. Therefore, the potential RIC-induced production of NO was also assessed. Levels of nitrite were measured in plasma as an indirect quantification of NO and no changes in plasma NO concentration were found following RIC (Fig. 1C). Likewise, neither age nor sex exerted any influence on NO levels in plasma (Supplementary Figs. 1E and F). Nevertheless, there is a trend of lower NO_2 levels in aged subgroup, which is in accordance with vascular aging process. In fact, vascular aging is associated with endothelial cell dyfunction along downregulation of eNOS and lower levels on NO, which in turn promotes vasoconstriction [32].

Circulating cell-free mitochondrial DNA (mtDNA) is also a biomarker of stress, being associated with inflammatory diseases, as well as with physical and psychological stress [33]. Therefore, mtDNA could emerge as a potential candidate for signalling minor stress and consequently RIC-induced cytoprotection. Nevertheless, no change was observed in total amount of cell-free mtDNA in plasma in response to RIC (Fig. 2D). When comparing young and senior subgroups, there was a significant difference in circulating mtDNA levels, with higher concentrations of mtDNA in the senior subgroup (Supplementary Fig. 1G). This observation may align with the increased levels of inflammatory markers associated with the aging process [33]. In contrast, no difference was observed between female and male subgroups (Supplementary Fig. 1H).

The critical role of glutathione (GSH) in defence against oxidative stress is well known, emphasizing the importance of maintaining a reduced cellular state through the regulated balance between synthesis and consumption of GSH and cysteine (Cys). Therefore, the distribution of low-molecular-weight thiols between tissues and plasma reflects oxidative stress [34]. RIC procedure was associated with an increase in the levels of GSH and cysteinylglycine (CysGly) bound to proteins (Fig. 3C and F) immediately after RIC; a decrease in the levels of total and free CysGly (Fig. 3D and E) 4h after RIC, while no alteration was observed in total or free forms of GSH (Fig. 3A and B). Furthermore, the levels of total, free or protein-bound forms of metabolites related to homocysteine (HCys) (Supplementary Figs. 2A–C) or of the GSH precursor Cys (Supplementary Figs. 2D–F) did not change in response to RIC.

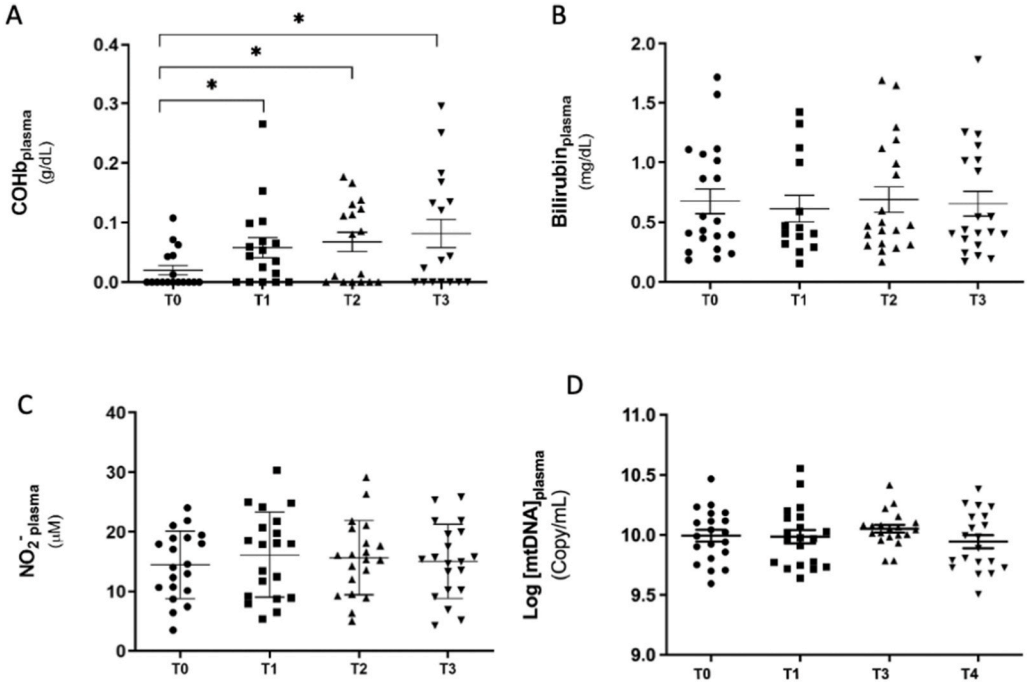

Fig. 2. Quantification of carbon monoxide (CO), bilirubin, nitric oxide (NO) and mitochondrial DNA in plasma before RIC (T0) and after RIC (T1, T2 and T3). (A) The amount of total Hb (g/dL) and the percentage of COHb were quantified by Avoximeter device, then the amount of COHb in g/dL was calculated. **(B)** After blood collection, plasma was separated and frozen at −80 °C for further quantification of bilirubin (mg/dL) using Bilirubin Assay Kit (Sigma Aldrich). **(C)** Griess reagent was used to measure plasma nitrite (NO_2), which is an indirect way to quantify NO. **(D)** Plasma was separated and frozen at −80 °C for further analysis of mitochondrial DNA (mtDNA) levels by quantitative PCR (Q-PCR). Values are represented as the logarithm of mtDNA copy number per mL of plasma. All values are mean ± SEM, n = 20 (n = 17 for COHb analysis) and data were analysed with the paired *t*-test, with * $p < 0.05$.

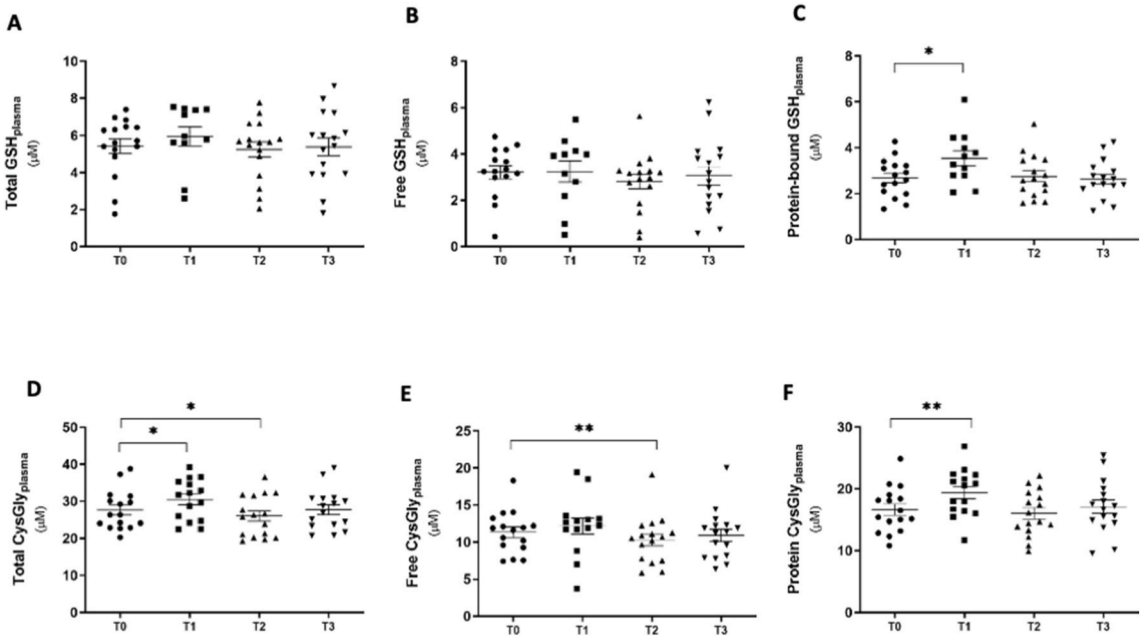

Fig. 3. Measurement of Glutathione (GSH) and its metabolite cysteinylglycine (CysGly) in plasma after RIC. GSH and CysGly were quantified in three different forms: free form, protein-bound form and total amount. Blood was collected from young and senior volunteers at T0, T1, T2 and T3, then plasma was separated and frozen at −80 °C for further analysis. Total GSH **(A)**, free GSH **(B)**, protein-bound GSH **(C)**, Total CysGly **(D)**, Free CysGly **(E)**, Protein-bound CysGly **(F)** were quantified by HPLC. Data are mean ± SEM, n = 16. Data were analysed using paired t tests with * $p < 0.05$ and **$p < 0.01$ compared with timepoint before RIC.

When the analysis was done with different age and sex subsets, no difference in response to RIC was found in the levels of GSH metabolites in senior, female or male groups (Supplementary Fig. 3). Moreover, no difference in the glutathiomic profile was observed between female and male subgroups (Supplementary Fig. 3).

In young group RIC also induced an increase in the levels of cysteines (Cys) and CysGly bound to proteins (Supplementary F ig. 3 F and L) and, accordingly a decrease in free Cys and CysGly (Supplementary F ig. 3 E and K). In healthy individuals, there is a recognized decline in S-cysteinylglycinylated and S-glutathionylated proteins with aging [35], which was also observed herein with a reduction of protein bound GSH in senior subset (Supplementary Fig. 3C). This decline has been described as a sign of a less efficient antioxidant defence system that comes with age, potentially contributing to an elevated risk of irreversible oxidation of proteins in plasma. Our findings suggest that in healthy volunteers RIC produces an inverted aging pattern by a rapid enhancement of plasma antioxidant capacity. Similarly to the complete pool of subjects, total CysGly levels also decreased in response to RIC (Supplementary Fig. 3D); and free HCys levels reduced after RIC in young subjects (Supplementary Fig. 3H), which may indicate an increase on GSH anabolism. In summary the anti-oxidant capacity is highly dependent on a shift in the delicate balance between various redox pools of thiols, in particular GSH and CysGly (Fig. 3).

Aiming to identify any RIC-induced response in plasma, all the above mentioned biochemical parameters were analysed by Principal Component Analysis (PCA). Score plots are a useful representation of the PCA, since they represent the samples (the human volunteers) according to the first two components of the PCA model. The first two components are new variables built with the data provided and explain the largest and second largest variation of the data, respectively. PCA did not reveal a distinct cluster at any of the timepoints after RIC when compared to before RIC. Likewise, no sex-related cluster was observed before RIC procedure (Supplementary Fig. 4A) or with all timepoints (Supplementary Fig. 4B). In contrast, the biochemical parameters globally differed between Young and Senior subgroups (Supplementary Fig. 4C), even pre-RIC (Supplementary Fig. 4D), wherein the factors contributing most to this distinction were plasma NO, the protein-bound form of GSH and mtDNA. This is not surprising once senior subjects present several comorbidities (Supplementary Table 1).

3.3. Proteomic analysis of plasma following RIC procedure

Alterations in the circulating protein pattern in plasma following RIC procedure were analysed after 4 (T2) and 22 (T3) hours by mass spectrometry in order to identify potential candidates for the observed beneficial effects of RIC [4]. A total of 828 proteins were identified of which 707 proteins, detected in at least 5 of the 10 subjects and in at least one of the time points in young or senior subjects, were used for downstream analysis. Fig. 4 schema outlines the statistical analysis procedure, the groups and the comparisons.

Significance was detected by paired Student's t-test comparisons between time points T0 (before RIC) versus T2 (4h after RIC) and T0 versus T3 (22h after RIC) for all 20 subjects and within 8 subsets: 10 young (10Y), 10 senior (10S), 11 female (11F), 9 male (9M),6 female senior (6FS), 5 female young (5FY), 4 male senior (4MS) and 5 male young (5MY) (see all results in Supplementary Table 2). No significance was detected after correction of p-values for multiple protein comparisons using Benjamini-Hochberg (BH) procedure. Data from proteins with p-values <0.05 (without BH correction) were further analysed using repeated measures one way-ANOVA over T0, T2 and T3 time points and Holm adjusted pairwise p-values determined between time points (Fig. 4). Volcano plots for visualization of overall data significance and fold change are shown in Fig. 5 for the sets and comparisons where the later analysis yielded significant p-values (ANOVA p-values <0.05 and paired p-value Holm-adj <0.05). Individual protein violin plots are shown in Fig. 6; fold change, significance, sets and comparisons are summarised in Table 1A. At 4 h after RIC this analysis only detected one increased protein in male subset (AXL, Log2 FC = 1.3) and one decreased protein in the young female subset (GLIPR2, Log2 FC = −2.6). At 22h after RIC, differences were observed in seven proteins. Two proteins were increased in set of all subjects (OSCAR, Log2 FC = 4.6; and LRIG3, Log2 FC = 3.9); OSCAR was also increased in male subset (Log2

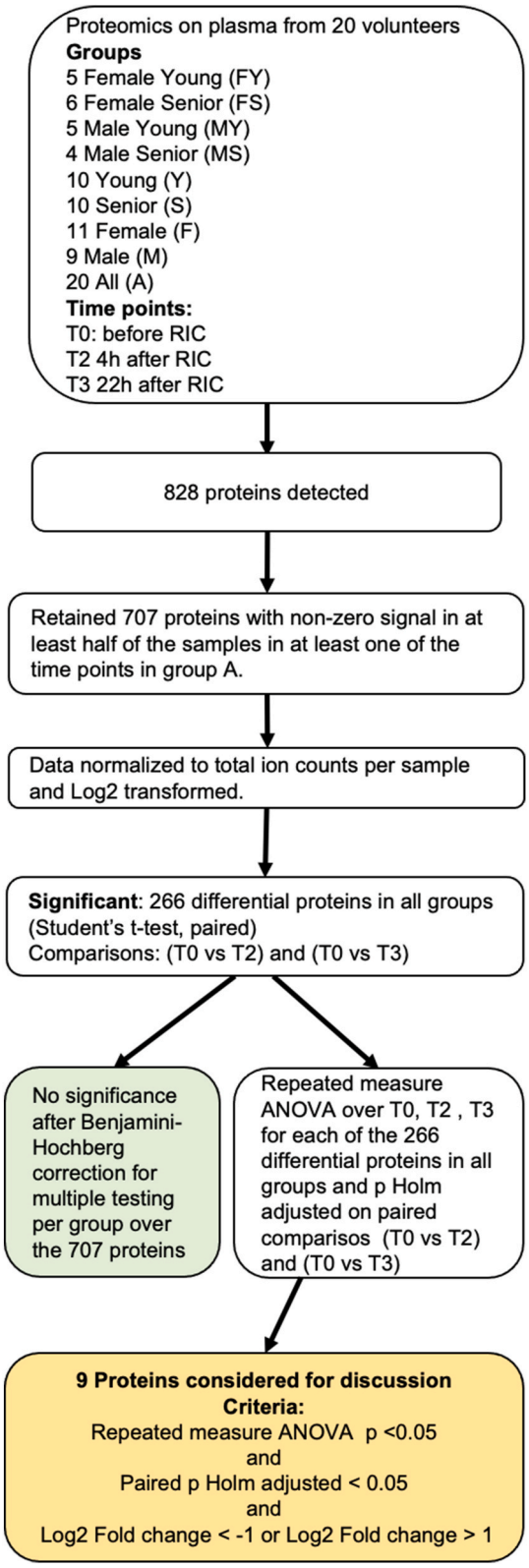

Fig. 4. Schema of proteomic analysis. The schema outlines the statistical analysis procedure, the groups and the comparisons.

FC = 8.3) and LRIG3 in senior subset (Log2 FC = 7.6) but not in the other subsets. In the male subset, in addition to the increase in OSCAR we also detected a reduction of LDHA (Log2 FC = −1.3), whereas in the senior subset, in addition to the increased LRIG3 we detected a substantial decrease in FBP1 (Log2 FC = −7.3). In the female subset we detected a reduced level of TPM3 (Log2 FC = −1) which is also seen in senior females (Log2 FC = −1.7). Finally in the young subset we detected a decrease in C4BPA (Log2 FC = −1.0) and in the young female subset a decrease in FAM3C (Log2 FC = −1.2). The coefficient of determination indicating Bayesian effect size is ranked as "Substantial" for all proteins in repeated measures ANOVA analysis (Fig. 6) giving strength to the explanatory power of our model.

Functional analysis of all 9 proteins for gene ontology annotations revealed that all 9 proteins are present either in the extracellular exosome and or the extracellular space (Table 1B), validating the location of the proteins and indicating that the extracellular exosome may be an important mechanism in the conditioning response, communicating the incidence of ischemia to other organs.

The lack of overlap in protein levels between young and senior subjects at either the early or the late responses, is in accordance with PCA analysis.

3.4. *Functional validation of RIC-conditioned plasma in human cell cultures*

The functional validation of whether RIC-conditioned plasma has any beneficial effects was obtained on various human cell models, including neurons, microglia, and brain microvasculature endothelial cells. The human neuron-like SH-SY5Y cell line was used after neuronal differentiation, along with the microglial human HCM3 cell line and the blood-brain barrier microvasculature endothelial cell line hCMEC/D3, which was also differentiated to form an endothelial barrier. Cells were cultured in the presence of FBS as a control, or with pooled human plasma derived from 10 young volunteers at each specified time point.

In order to disclose any neuroprotective role of conditioned plasma, neuronal morphology and synaptophysin expression were assessed as indirect measures of neuronal function. SH-SY5Y differentiated neuronal cells were cultured in the presence of human plasma derived from different time points after RIC. β-tubulin III immunostaining was used to quantify the number of neurites and to normalize it to the number of cells assessed by nuclear staining with DAPI (Fig. 7A). No difference in total area of neurites was found under different treatments (Fig. 7B). In contrast, neuronal culture supplemented with RIC-conditioned plasma appears to present a tendency of increased synaptophysin expression, particularly at later time points (Fig. 7C and Supplementary Fig. 5). In summary, although there was no detectable increase in neurite number, RIC-conditioned plasma may contain some factors that improve synapse formation. The potential for RIC-mediated neuroprotection was also assessed by cell viability. SH-SY5Y cells were cultured with human plasma or FBS supplemented media 24h before inducing cell death with the pro-oxidant molecule *tert*-butyl-hydroperoxide. Human plasma supplementation appeared to protect SH-SY5Y cells against cell death compared to control conditions (Fig. 7D). Therefore, human plasma *per se* protects neurons against cell death, but there appears to be no specific additional effect of RIC on neuronal cell death response.

Microglia are key glial cells in the response against stroke due to their role in inflammation control and phagocytosis. Herein, production of ROS was used as a measure of inflammatory response of microglia. HMC3 cells were cultured with media supplemented with FBS or with human plasma conditioned or not by RIC. Cells were then challenged with LPS and ATP to trigger neuroinflammation. In the absence of inflammatory conditions, exposure to human plasma led to a reduction in the baseline levels of ROS production (Fig. 8A). Upon inflammatory challenge, cells treated with human plasma exhibited lower levels of ROS compared to the control conditions. Thus, RIC might induce changes in plasma composition that mitigate neuroinflammation. Interestingly, whenever conditioned plasma was tested in murine microglial BV-2 cell line the same anti-neuroinflammatory effect was also observed for plasma derived from young subjects, further supporting its anti-neuroinflammatory action in another cell model

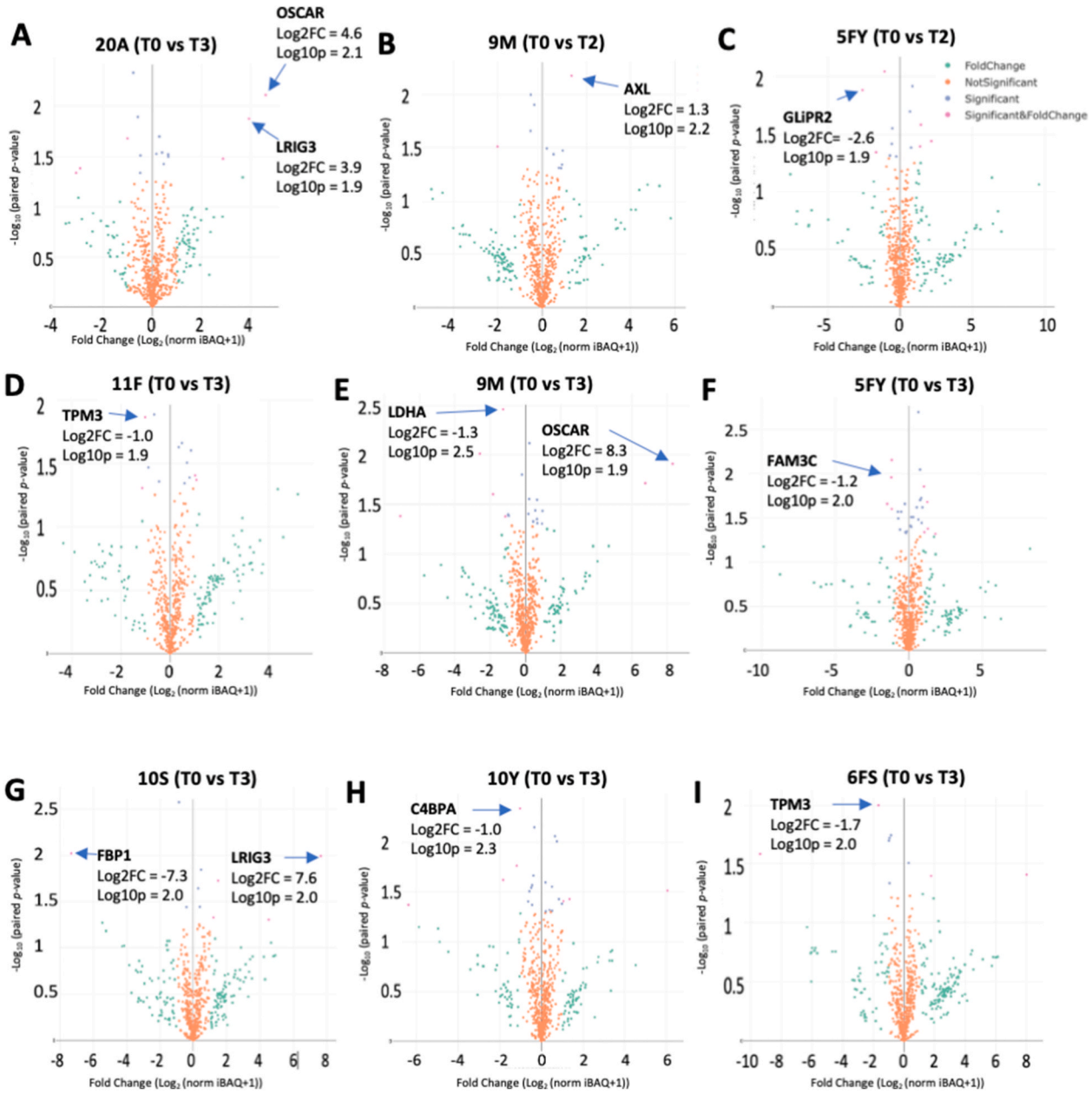

Fig. 5. Volcano plot analysis and visualization of proteomics data. Volcano plots for visualization of overall data significance and fold change for the sets and comparisons. The Y axis is -Log10 (paired p-Value) and the X axis is FC Log2(normiBAQ+1). The highlighted proteins present significant p-values (ANOVA p-values <0.05 and paired p-value Holm-adj <0.05). **(A)** all 20 subjects with T0 and T3 comparison; **(B)** 9 male subjects with T0 and T2 comparison **(C)** 5 female young subjects with T0 and T2 comparison; **(D)** 11 female subjects with T0 and T3 comparison; **(E)** 9 male subjects with T0 and T3 comparison; **(F)** 5 female young subjects with T0 and T3 comparison; **(G)** 10 senior subjects with T0 and T3 comparison; **(H)** 10 young subjects with T0 and T3 comparison and **(I)** 6 female senior subjects with T0 and T3 comparison.

(Supplementary Fig. 6). Nevertheless no anti-inflammatory role of RIC-conditioned plasma was found for plasma derived from senior, female or male subgroups (Supplementary Fig. 6).

The analysis of the endothelial blood-brain barrier (BBB), formed by the differentiated hCMEC D3 cell line, involved the assessment of the permeability coefficient using Lucifer yellow dye. In comparison to the control with FBS, the presence of human plasma resulted in a decreased permeability coefficient, indicative of enhanced protection for BBB by improving its integrity.

However, it is noteworthy that permeability coefficients observed for both non-conditioned plasma and conditioned plasma at later RIC timepoints were found to be similar, suggesting that no BBB protection is promoted by RIC (Fig. 8B). The same was observed when RIC-conditioned plasma from senior, female or male subsets were used (Supplementary Fig. 7).

4. Discussion

For the first time, biochemical characterization and proteomic analysis were performed after RIC procedure in healthy human subjects (not in stroke patients) for the identification of circulating molecules that may be implicated in the neuroprotective function induced by RIC. In contrast to previous studies in the literature, our main objective was to characterize RIC response in subjects without stroke. Because stroke is an age-associated disease, two subsets of individuals were studied: young and senior. In contrast to young subjects, who are indeed healthy

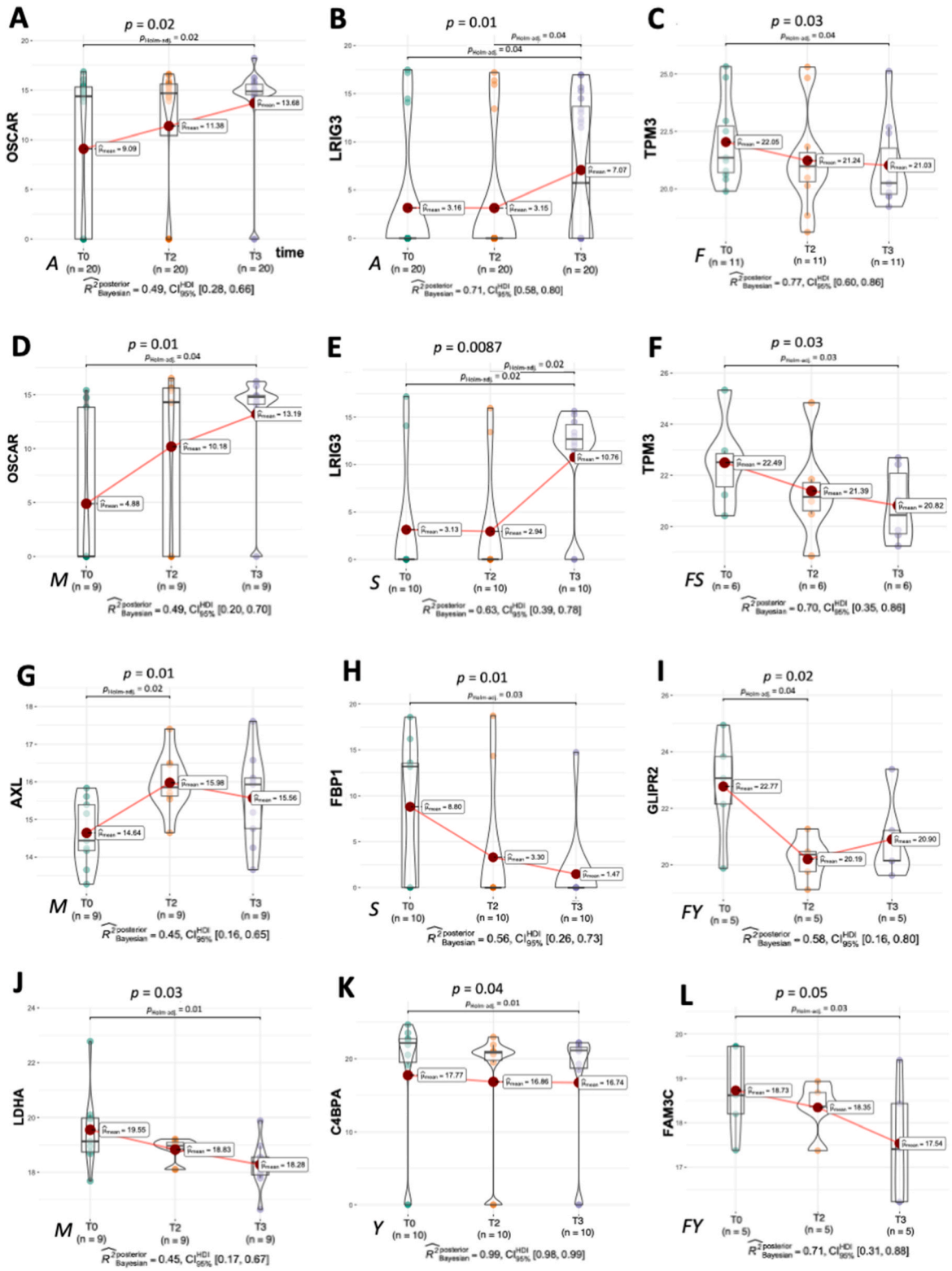

Fig. 6. Individual protein violin plots. Variation on protein levels over time is presented as violin plots with ANOVA p-values, paired p-value Holm-adj and the coefficient of determination that indicates Bayesian effect size. **(A)** OSCAR for all individuals; **(B)** LRIG3 for all individuals; **(C)** TPM3 for female subgroup; **(D)** OSCAR for male subgroup; **(E)** LRIG3 for senior subgroup; **(F)** TPM3 for female senior subgroup; **(G)** AXL for male subgroup; **(H)** FBP1 For senior subgroup; **(I)** GLIPR2 for female young subgroup; **(J)** LDHA for male subgroup; **(K)** C4PBA for young group and **(L)** FAM3C for female young subgroup.

individuals, the senior volunteers present age-associated comorbidities, which can influence the RIC response. Nevertheless, it is also extremely relevant to show that results observed in young may be overhauled by the confounding morbidities in the senior population, for which this study is ultimately targeted. In fact, the biochemical pattern and the proteomic analysis revealed to be different in the two subgroups.

Several biochemical tests were done in plasma or blood for the quantification of NO, CO, bilirubin, free mtDNA or GSH and its

Table 1
RIC-induced alterations in circulating proteins. (A) List of proteins differentially present in plasma after RIC. Red color represents an increase on protein concentration in plasma following RIC procedure, while green color means a reduction on protein levels. **(B)** Gene ontology annotations of 9 proteins differently present in plasma following RIC.

A

Comparison	Set	Protein GeneSymbol	Protein	Repeated measures ANOVA p	Paired p (Holm-adj) T0 vs T2	Log2 FC (T0 vs T2)	Paired p (Holm-adj) T0 vs T3	Log2 FC (T0 vs T3)
T0 vs T2	Male	AXL	Receptor tyrosine kinase	**	*	1.3	#	<1
T0 vs T2	Female Young	GLIPR2	Glioma pathogenesis related-2	*	*	-2.6	ns	<1
T0 vs T3	All	OSCAR	Osteoclast-associated receptor	*	ns	<1	*	4.6
T0 vs T3	All	LRIG3	Leucine-rich repeats and immunoglobulin-like domains protein 3	**	ns	<1	*	3.9
T0 vs T3	Female	TPM3	Tropomyosin 3	*	ns	<1	*	-1.0
T0 vs T3	Male	LDHA	Lactate deshydrogenase A	*	ns	<1	*	-1.3
T0 vs T3	Male	OSCAR	Osteoclast-associated receptor	**	ns	<1	*	8.3
T0 vs T3	Senior	FBP1	Fructose-bisphosphatase 1	**	#	<1	*	-7.3
T0 vs T3	Senior	LRIG3	Leucine-rich repeats and immunoglobulin-like domains protein 3	**	ns	<1	*	7.6
T0 vs T3	Female Senior	TPM3	Tropomyosin 3	*	ns	<1	*	-1.7
T0 vs T3	Young	C4BPA	C4b-binding protein alpha chain	*	ns	<1	*	-1.0
T0 vs T3	Female Young	FAM3C	Metabolism regulating signaling molecule C	*	ns	<1	*	-1.2

B

Gene Ontology Term (Cellular Component)	PValue	Genes	Fold Enrichment	FDR
GO:0070062~extracellular exosome	3.66E-05	FBP1, LDHA, OSCAR, TPM3, AXL, FAM3C, GLIPR2	7.2	0.00102487
GO:0005615~extracellular space	4.54E-03	AXL, FAM3C GLIPR2, C4BPA, LRIG3	5.7	0.06358001

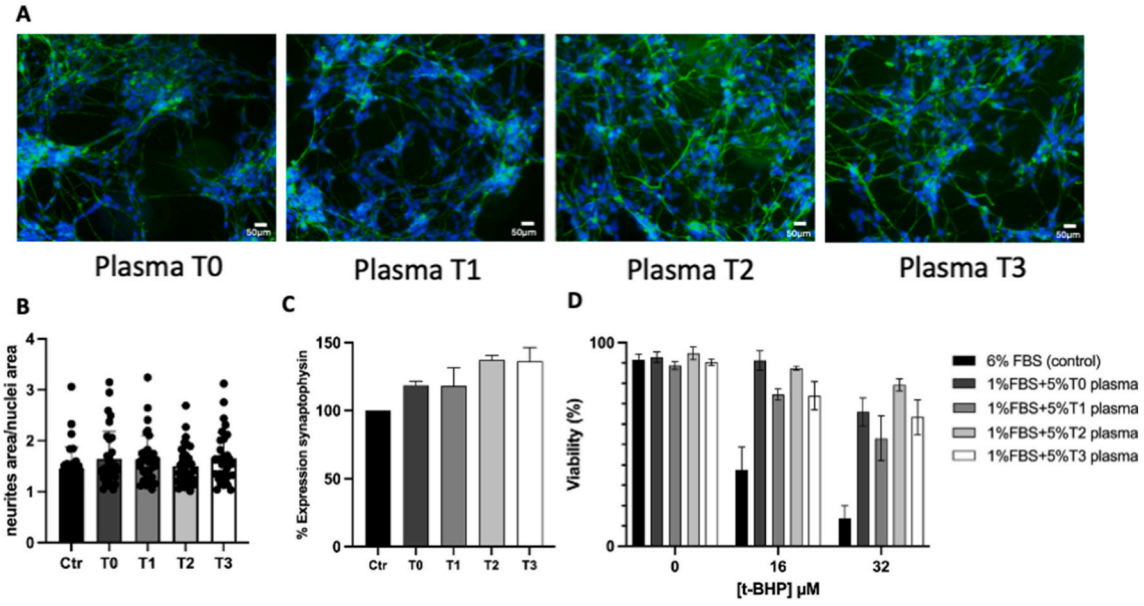

Fig. 7. Functional assessment of conditioned plasma in neuron-like cells. SH-SY5Y cells were differentiated for 6 days in the presence of 1 % FBS and retinoic acid, followed by medium exchange for: 6 % of FBS (control), 1 % of FBS with 5 % of human plasma at different time points before RIC procedure (T0) and T1, T2 and T3 after RIC. **(A)** Representative images for the characterization of SH-SY5Y neuron-like cells by immunocytochemistry (green staining: β-tubulin III; blue staining: DAPI). **(B)** Quantification of neurite area (β-tubulin III staining) normalized by nuclei area under the 5 different conditions. **(C)** Quantification of synaptophysin by Western blot following treatment with different plasma samples; expression of synaptophysin in control cells is considered 100 %. **(D)** For viability tests, medium of non-differentiated SH-SY5Y cells were exchanged by 5 % FBS with 5 % non-conditioned human plasma (T0) or with conditioned plasma at different time points (T1, T2 and T3) for 24h, then cells were challenged with prooxidant t-BHP at 16 or 32 µM for 18h and cell viability was assessed by flow cytometry using propidium iodide. Data are mean ± SEM, n ≥ 4.

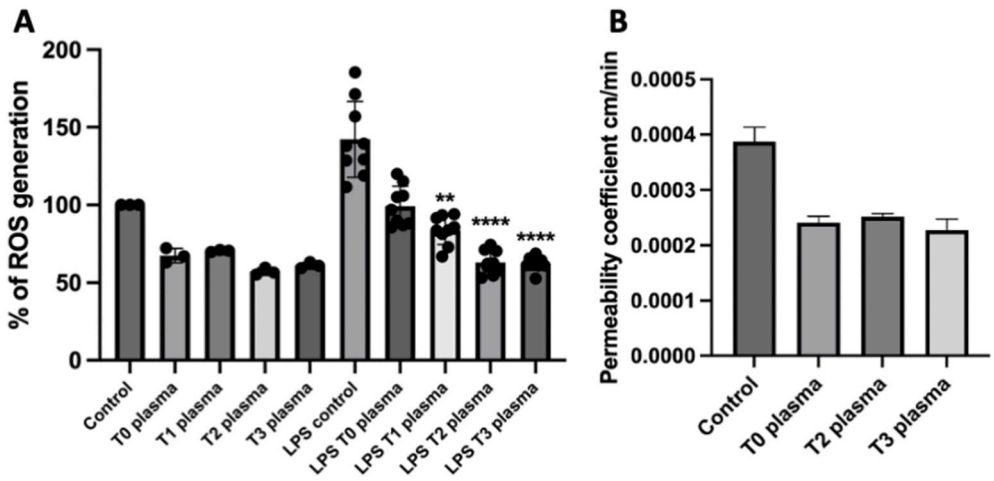

Fig. 8. Functional assessment of conditioned plasma in neuroinflammatory response of human microglial HMC3 cells and in permeabilization of human brain microvasculature endothelial cells hCMEC D3 – BBB model. (A) HMC3 cells were cultured for 24h in medium containing: 11 % FBS (control), 6 % FBS plus 5 % of non-conditioned human plasma (T0) or 6 % FBS plus 5 % conditioned human plasma (T1, T2 and T3). LPS was added for 24h and ATP was then added for another 30 min for stimulation of inflammation. Intracellular ROS (mainly more reactive products derived from H_2O_2 oxidation) generation was quantified with the fluorescent dye H_2DCFDA. Values are mean ± SEM, n = 9. Data were analysed using unpaired t tests with $^{**}p < 0.01$ and $^{****}p < 0.0001$ compared with non-conditioned plasma (T0). **(B)** hCMEC D3 cells were differentiated in inserts for 11 days and their permeability was tested using Lucifer yellow dye passage. hCMEC D3 cells were cultured for 24h in medium containing: 7.5 % FBS (control), 2.5 % FBS plus 5 % non-conditioned human plasma (T0) or 2.5 % FBS plus 5 % conditioned human plasma (T2 and T3). Permeability coefficient was calculated based on the passage of dye through endothelial cell barrier after 45 min. Values are mean ± SEM, n = 3.

metabolites. Blood CO levels (assessed by COHb formation) increased following RIC at all time points and in a time-response manner. Accordingly, CO is endogenously produced by haem-oxygenase, which is a stress response enzyme that is upregulated (HO-1 inducible isoform) or activated (HO-2 constitutive isoform) in response to different types of biological stresses, namely inflammation, hypoxia, oxidative stress, among others [36]. Likewise, CO at very low concentrations is also an important signalling gasotransmitter in the brain, being neuroprotective, anti-neuroinflammatory and maintaining BBB integrity [29]. Thus, one can speculate that the low stress generated by RIC promotes HO activity and generates CO at endothelial level, which in turn may be locally protective in different organs. Moreover, the assessment of COHb increased levels following RIC could be a useful rapid biomarker to evaluate the success of RIC-induced mild stress and potentially beneficial effects. Proteins bound to GSH and to CysGly also enhanced immediately after RIC, which may suggest a mechanism of protein protection against oxidative stress, in particular against irreversible oxidation of Cys residue in proteins [37]. CysGly is a metabolite of GSH, and both its total and free levels exhibited a decrease after RIC procedure, which might imply a reduction in the catabolism of GSH in response to RIC. The prooxidant role played by molecular species originating during GSH catabolism further support the impact of RIC increasing antioxidant responses [38]. Finally, the pattern of glutathione metabolites did not change in response to RIC in senior, female or male subgroups. This may occur because the sample size is small; or it can also be speculated that senior individuals present lower ability to respond against oxidative stress with glutathione metabolites.

The proteomic analysis revealed 9 proteins that are differently present in plasma following RIC. The circulating levels of osteoclast-associated receptor (OSCAR), Receptor tyrosine kinase (Axl) and Leucine-rich repeats and immunoglobulin-like domains protein 3 (LRIG3) increased in response to RIC. OSCAR is expressed in all cells of myeloid lineage, and is involved in osteoclast differentiation, the maturation of dendritic cells and modulates inflammatory response in monocytes and neutrophils [39,40]. OSCAR is also present in human vascular endothelial cells and is activated by oxidized low density lipoproteins (oxy-LDL) promoting inflammatory response [41]. Thus, OSCAR could play a role in modulating inflammation in the vasculature induced by RIC, potentially triggering a systemic protective response. Axl receptor tyrosine kinase is expressed in endothelial cells and vascular smooth muscle cells, and can be cleaved releasing soluble protein in plasma [42]. Moreover, Axl circulating levels increase in response to hypoxia or vascular injury, modulating inflammation [42]. Interestingly in cancer cells Axl prevents apoptosis and regulates angiogensis and cell proliferation, and its expression increases in response to hypoxia [43,44]. Thus RIC-increased Axl levels in plasma is in accordance with hypoxic response, inflammatory control and potential inhibition of apoptosis. The leucine rich repeats and immunoglobulin like domains 3 protein (LRIG3) is considered a tumour suppressor since its expression triggers apoptosis, inhibits cell adhesion and invasion/migration of tumour cells and modulates inflammation [45]. In fact, LRIG3 appears to suppress cell growth in glioblastoma, being a potential prognostic biomarker in glioblastomas [46], as well as in other cancer types [47].

In contrast, RIC procedure reduced the circulation level of 6 proteins: Glioma pathogenesis related-2 (GLIPR2), Tropomyosin 3 (TPM3), Lactate deshydrogenase A (LDHA), Fructose-bisphosphatase 1 (FBP1), C4b-binding protein alpha chain (C4BPA) and Metabolism regulating signalling molecule C (FAM3C).

GLIPR2 is a Golgi-associated protein that reduces autophagic process in several different models by inhibiting the activity of the class III phosphatidylinositol 3-kinase complex I (PtdIns3K–C1) [48]. Thus, a decrease on its levels might promote autophagy which can be a cytoprotective process for elimination of dysfunctional cells or organelles. Furthermore, in a model of pulmonary fibrosis triggered by Paraquat, downregulation of GLIPR2 reduces the oxidative stress-induced epithelial-mesenchymal transition [49]. This data indicates that RIC-induced reduction of GLIPR2 levels in circulation may be beneficial. The expression of TPM3 is higher in esophageal squamous cell carcinoma [50] and in ovarian cancer patients [51]. In contrast, expression of TPM3 attenuates hypoxia-induced cell damage and oxidative stress in cardiomyocytes [52]. LDHA is a subunit of the cytosolic enzyme operating the inter-conversion of pyruvate and L-lactate with rescue recycling of NADH to NAD+ in hypoxia [53]. In cancer cells, the metabolic shift towards glycolysis (Warburg effect) requires LDHA activity, thus inhibition or downregulation of LDHA promotes apoptosis of cancer

cells [54]. Whether a decrease of glycolysis is a cytoprotective effect of RIC remains to be further studied. Interestingly, in an experimental mouse model of cerebral ischemia, administration of arginine decreases HIF-1α/LDHA-mediated inflammation, promoting neuroprotection [55], thus one may speculate that RIC could protect by limiting LDHA-induced neuroinflammation.

FBP1 is a gluconeogenesis regulatory enzyme and plays a key role in control of metabolism in pancreas and liver, being involved in glucose homeostasis. Recently it was shown that in the model of hindlimb ischemia, angiogenesis is stimulated by increasing endothelial glycolysis via downregulation of FBP1 expression [56]. Likewise, RIC procedure may also trigger angiogenesis in response to the lack of blood supply by decreasing FBP1 expression. Moreover, in an inflammatory asthma model, downregulation of FBP1 expression decreases oxidative stress, apoptosis and inflammation (namely interleukin (IL)-4- and IL-13), conversely overexpression of FBP1 aggravates oxidative stress and apoptosis by suppressing Nfr2 activation [57]. Thus, one can speculate that lower circulating level of FBP1 indicates a potential molecular mechanism of RIC to be protective, as it is also present in the extracellular exosome. FAM3C is a biomarker for poor prognosis is several cancers and is involved in the epithelial-to-mesenchymal transition [58,59]. Accordingly, ubiquitous overexpression of FAM3C in mouse decreased lifespan and body weight and induced anaemia and liver fibrosis [60]. Therefore FAM3C reduced concentrations in plasma could indicate a beneficial effect of RIC. Finally, C4BPA was the first circulating complement regulatory protein identified and it functions as an important complement inhibitor by binding to several ligands including heparin, C-reactive protein or CD40. C4BPA prevents the complement cascade from attacking host cells by binding to the complement cleavage products C4b and C3b. The fact that RIC decreases plasma levels of C4BPA may indicate that it may facilitate innate immune response and inflammation. Interestingly, in cortical-subcortical ischemic stroke, levels of C4BPA are higher, which may be speculated as a biomarker of brain tissue damage [61].

The analysed circulating proteins provide insights into the mode of action of RIC. The circulating protein alterations in young subgroups may be more representative of the underlying mechanisms of RIC since in these subjects there is no influence of ageing and/or co-morbidities. Probably the most striking observation is that no protein overlaps were found in the different age and sex subsets, which, although the number of subjects is limited, may emphasise the importance of sex and age being major personalized differentiating criteria to consider if RIC were to be implemented as a protective strategy against stroke. Furthermore, our results also indicate that age significantly affects plasma biochemical parameters. Increasing the number of subjects in future studies will enhance the robustness of these findings and in turn give a deeper understanding of the underlying mechanisms of RIC. These results highlight the need for specific studies to better comprehend the age and sex-specific impact of the RIC procedure by to analysing young, senior, male and female subgroups separately.

Functional validation of conditioned plasma was limited. In fact, conditioned plasma protected against inflammation assessed by ROS generation only when applied to human microglia. In neurons, conditioned plasma showed a trend to increase synaptophysin expression suggesting an enhancement of neuronal signalling, although it was not statistically significant. Unexpectedly, no effect was found in the permeability of human brain microvasculature endothelial cells, which would be the first gate for brain protection supported by blood circulating molecules.

The RIC-induced alterations in circulating factors and proteins and their potential functional action on human cells *in vitro* appears limited. However, taking into account the fact that RIC is a mild procedure, promoting low levels of stress, one would expect a mild response to be associated with RIC. Therefore, one can speculate that in order to have a stronger effect, RIC should be applied in a more chronic fashion, namely daily for one week or for a month. In fact, a clear protective effect of RIC in stroke patients was only found when RIC was applied daily for 14 days following stroke [62]. Thus, further mechanistic studies are needed with long term and repeated RIC applications in order to identify sustained levels of blood biochemical factors involved in the inter-organ communication and neuroprotection. In addition, RIC procedure can also be envisaged as a preventive chronic therapy rather than an acute phase therapy. Concerning cerebral disorders, RIC may also have therapeutic potential for chronic diseases such as vascular dementia or neurodegenerative diseases, besides stroke or brain traumatic injury.

In conclusion, although RIC presents beneficial effect in experimental models and clinical trials, more studies in human subjects are needed to disclose the molecular mechanisms underlying RIC. In particular, it is necessary to test RIC procedure in a chronic (repetitive) manner to assess sustained changes in putative beneficial blood biomarkers.

Source of funding

The funding agency that supported the work “Fundação para a Ciência e Tecnologia” (FCT) Portugal, with four projects: Applied Molecular Biosciences Unit-UCIBIO (UID/Multi/04378/2019), iNOVA4-Health - Programme in Translational Medicine (UID/Multi/04462/2013), LA/P/0140/2020 of the Associate Laboratory Institute for Health and Bioeconomy and PTDC/MEC-NEU/28,750/2017 and the PhD scholarship for NLS (PD/BD/127,819/2016).

CRediT authorship contribution statement

Inês G. Mollet: Writing – review & editing, Writing – original draft, Methodology, Investigation, Formal analysis, Data curation. **Ricardo Viana-Soares:** Writing – review & editing, Methodology, Investigation, Data curation. **Catarina Cardoso-Pires:** Validation, Methodology, Investigation, Formal analysis. **Nuno L. Soares:** Methodology, Investigation, Data curation. **João Pedro Marto:** Validation, Methodology, Investigation, Conceptualization. **Marcelo Mendonça:** Writing – review & editing, Investigation, Conceptualization. **Cláudia S.F. Queiroga:** Writing – review & editing, Methodology, Investigation, Conceptualization. **Ana S. Carvalho:** Writing – review & editing, Methodology, Investigation, Formal analysis. **Catarina O. Sequeira:** Methodology, Investigation. **Luísa Teixeira-Santos:** Writing – review & editing, Methodology, Formal analysis. **Tatiana P. Fernandes:** Methodology, Data curation. **Kerman Aloria:** Methodology. **Sofia A. Pereira:** Writing – review & editing, Methodology, Investigation. **Rune Matthiesen:** Methodology, Investigation. **Miguel Viana-Baptista:** Writing – review & editing, Supervision, Funding acquisition, Conceptualization. **Helena L.A. Vieira:** Writing – review & editing, Validation, Supervision, Resources, Methodology, Investigation, Funding acquisition, Formal analysis, Conceptualization.

Declaration of competing interest

On the behalf of all authors, I declare no conflict of interest.

Acknowledgments

The authors would like to acknowledge the association: “Liga dos Amigos do Hospital Sao Francisco Xavier” from “Centro Hospitalar Lisboa Ocidental”. We also thank Flow Cytometry Facility of NMS-UNL, as well as UCIBIO’s BioLabs, NOVA-FCT-UNL.

Appendix A. Supplementary data

Supplementary data to this article can be found online at https://doi.org/10.1016/j.freeradbiomed.2024.08.017.

References

[1] C.E. Murry, R.B. Jennings, K.A. Reimer, Preconditioning with ischemia: a delay of lethal cell injury in ischemic myocardium, Circulation 74 (1986) 1124–1136, https://doi.org/10.1161/01.CIR.74.5.1124.

[2] U. Dirnagl, K. Becker, A. Meisel, Preconditioning and tolerance against cerebral ischaemia: from experimental strategies to clinical use, Lancet Neurol. 8 (2009) 398–412.

[3] D.C. Hess, R.a. Blauenfeldt, G. Andersen, K.D. Hougaard, M.N. Hoda, Y. Ding, X. Ji, Remote ischaemic conditioning-a new paradigm of self-protection in the brain, Nat. Rev. Neurol. 11 (2015) 698–710, https://doi.org/10.1038/nrneurol.2015.223.

[4] I. Mollet, J.P. Marto, M. Mendonça, M.V. Baptista, H.L.A. Vieira, Remote but not distant: a review on experimental models and clinical trials in remote ischemic conditioning as potential therapy in ischemic stroke, Mol. Neurobiol. 59 (2022) 294–325, https://doi.org/10.1007/s12035-021-02585-6.

[5] J.M.J. Pickard, H.E. Bøtker, G. Crimi, B. Davidson, S.M. Davidson, D. Dutka, P. Ferdinandy, R. Ganske, D. Garcia-Dorado, Z. Giricz, A.V. Gourine, G. Heusch, R. Kharbanda, P. Kleinbongard, R. MacAllister, C. McIntyre, P. Meybohm, F. Prunier, A. Redington, N.J. Robertson, M.S. Suleiman, A. Vanezis, S. Walsh, D. M. Yellon, D.J. Hausenloy, Remote ischemic conditioning: from experimental observation to clinical application: report from the 8th Biennial Hatter Cardiovascular Institute Workshop, Basic Res. Cardiol. 110 (2015) 453, https://doi.org/10.1007/s00395-014-0453-6.

[6] V.L. Feigin, B.A. Stark, C.O. Johnson, G.A. Roth, C. Bisignano, G.G. Abady, M. Abbasifard, M. Abbasi-Kangevari, F. Abd-Allah, V. Abedi, A. Abualhasan, N. M. Abu-Rmeileh, A.I. Abushouk, O.M. Adebayo, G. Agarwal, P. Agasthi, B. O. Ahinkorah, S. Ahmad, S. Ahmadi, Y. Ahmed Salih, B. Aji, S. Akbarpour, R. O. Akinyemi, H. Al Hamad, F. Alahdab, S.M. Alif, V. Alipour, S.M. Aljunid, S. Almustanyir, R.M. Al-Raddadi, R. Al-Shahi Salman, N. Alvis-Guzman, R. Ancuceanu, D. Anderlini, J.A. Anderson, A. Ansar, I.C. Antonazzo, J. Arabloo, J. Ärnlöv, K.D. Artanti, Z. Aryan, S. Asgari, T. Ashraf, M. Athar, A. Atreya, M. Ausloos, A.A. Baig, O.C. Baltatu, M. Banach, M.A. Barboza, S.L. Barker-Collo, T. W. Bärnighausen, M.T.U. Barone, S. Basu, G. Bazmandegan, E. Beghi, M. Beheshti, Y. Béjot, A.W. Bell, D.A. Bennett, I.M. Bensenor, W.M. Bezabhe, Y.M. Bezabih, A. S. Bhagavathula, P. Bhardwaj, K. Bhattacharyya, A. Bijani, B. Bikbov, M. M. Birhanu, A. Boloor, A. Bonny, M. Brauer, H. Brenner, D. Bryazka, Z.A. Butt, F. L. Caetano dos Santos, I.R. Campos-Nonato, C. Cantu-Brito, J.J. Carrero, C. A. Castañeda-Orjuela, A.L. Catapano, P.A. Chakraborty, J. Charan, S.G. Choudhari, E.K. Chowdhury, D.-T. Chu, S.-C. Chung, D. Colozza, V.M. Costa, S. Costanzo, M. H. Criqui, O. Dadras, B. Dagnew, X. Dai, K. Dalal, A.A.M. Damasceno, E. D'Amico, L. Dandona, R. Dandona, J. Darega Gela, K. Davletov, V. De la Cruz-Góngora, R. Desai, D. Dhamnetiya, S.D. Dharmaratne, M.L. Dhimal, M. Dhimal, D. Diaz, M. Dichgans, K. Dokova, R. Doshi, A. Douiri, B.B. Duncan, S. Eftekharzadeh, M. Ekholuenetale, N. El Nahas, I.Y. Elgendy, M. Elhadi, S.I. El-Jaafary, M. Endres, A.Y. Endries, D.A. Erku, E.J.A. Faraon, U. Farooque, F. Farzadfar, A.H. Feroze, I. Filip, F. Fischer, D. Flood, M.M. Gad, S. Gaidhane, R. Ghanei Gheshlagh, A. Ghashghaee, N. Ghith, G. Ghozali, S. Ghozy, A. Gialluisi, S. Giampaoli, S. A. Gilani, P.S. Gill, E. V Gnedovskaya, M. Golechha, A.C. Goulart, Y. Guo, R. Gupta, V.B. Gupta, V.K. Gupta, P. Gyanwali, N. Hafezi-Nejad, S. Hamidi, A. Hanif, G. J. Hankey, A. Hargono, A. Hashi, T.S. Hassan, H.Y. Hassen, R.J. Havmoeller, S. I. Hay, K. Hayat, M.I. Hegazy, C. Herteliu, R. Holla, S. Hostiuc, M. Househ, J. Huang, A. Humayun, B.-F. Hwang, L. Iacoviello, I. Iavicoli, S.E. Ibitoye, O. S. Ilesanmi, I.M. Ilic, M.D. Ilic, U. Iqbal, S.S.N. Irvani, S.M.S. Islam, N.E. Ismail, H. Iso, G. Isola, M. Iwagami, L. Jacob, V. Jain, S.-I. Jang, S.K. Jayapal, S. Jayaram, R. Jayawardena, P. Jeemon, R.P. Jha, W.D. Johnson, J.B. Jonas, N. Joseph, J. J. Jozwiak, M. Jürisson, R. Kalani, R. Kalhor, Y. Kalkonde, A. Kamath, Z. Kamiab, T. Kanchan, H. Kandel, A. Karch, P.D. Katoto, G.A. Kayode, P. Keshavarz, Y. S. Khader, E.A. Khan, I.A. Khan, M. Khan, M.A. Khan, M.N. Khatib, J. Khubchandani, G.R. Kim, M.S. Kim, Y.J. Kim, A. Kisa, S. Kisa, M. Kivimäki, D. Kolte, A. Koolivand, S.L. Koulmane Laxminarayana, A. Koyanagi, K. Krishan, V. Krishnamoorthy, R. V Krishnamurthi, G.A. Kumar, D. Kusuma, C. La Vecchia, B. Lacey, H.M. Lak, T. Lallukka, S. Lasrado, P.M. Lavados, M. Leonardi, B. Li, S. Li, H. Lin, R.-T. Lin, X. Liu, W.D. Lo, S. Lorkowski, G. Lucchetti, R. Lutzky Saute, H. Magdy Abd El Razek, F.G. Magnani, P.B. Mahajan, A. Majeed, A. Makki, R. Malekzadeh, A.A. Malik, N. Manafi, M.A. Mansournia, L.G. Mantovani, S. Martini, G. Mazzaglia, M.M. Mehndiratta, R.G. Menezes, A. Meretoja, A. G. Mersha, J. Miao Jonasson, B. Miazgowski, T. Miazgowski, I.M. Michalek, E. M. Mirrakhimov, Y. Mohammad, A. Mohammadian-Hafshejani, S. Mohammed, A. H. Mokdad, Y. Mokhayeri, M. Molokhia, M.A. Moni, A. Al Montasir, R. Moradzadeh, L. Morawska, J. Morze, W. Muruet, K.I. Musa, A.J. Nagarajan, M. Naghavi, S. Narasimha Swamy, B.R. Nascimento, R.I. Negoi, S. Neupane Kandel, T.H. Nguyen, B. Norrving, J.J. Noubiap, V.E. Nwatah, B. Oancea, O.O. Odukoya, A. T. Olagunju, H. Orru, M.O. Owolabi, J.R. Padubidri, A. Pana, T. Parekh, E.-C. Park, F. Pashazadeh Kan, M. Pathak, M.F.P. Peres, A. Perianayagam, T.-M. Pham, M. A. Piradov, V. Podder, S. Polinder, M.J. Postma, A. Pourshams, A. Radfar, A. Rafiei, A. Raggi, F. Rahim, V. Rahimi-Movaghar, M. Rahman, M.A. Rahman, A. M. Rahmani, N. Rajai, P. Ranasinghe, C.R. Rao, S.J. Rao, P. Rathi, D.L. Rawaf, S. Rawaf, M.B. Reitsma, V. Renjith, A.M.N. Renzaho, A. Rezapour, J.A. B. Rodriguez, L. Roever, M. Romoli, A. Rynkiewicz, S. Sacco, M. Sadeghi, S. Saeedi Moghaddam, A. Sahebkar, K. Saif-Ur-Rahman, R. Salah, M. Samaei, A.M. Samy, I. S. Santos, M.M. Santric-Milicevic, N. Sarrafzadegan, B. Sathian, D. Sattin, S. Schiavolin, M.P. Schlaich, M.I. Schmidt, A.E. Schutte, S.G. Sepanlou, A. Seylani, F. Sha, S. Shahabi, M.A. Shaikh, M. Shannawaz, M.S.R. Shawon, A. Sheikh, S. Sheikhbahaei, K. Shibuya, S. Siabani, D.A.S. Silva, J.A. Singh, J.K. Singh, V. Y. Skryabin, A.A. Skryabina, B.H. Sobaih, S. Stortecky, S. Stranges, E.G. Tadesse, I. U. Tarigan, M.-H. Temsah, Y. Teuschl, A.G. Thrift, M. Tonelli, M.R. Tovani-Palone, B.X. Tran, M. Tripathi, G.W. Tsegaye, A. Ullah, B. Unim, B. Unnikrishnan, A. Vakilian, S. Valadan Tahbaz, T.J. Vasankari, N. Venketasubramanian, D. Vervoort, B. Vo, V. Volovici, K. Vosoughi, G.T. Vu, L.G. Vu, H.A. Wafa, Y. Waheed, Y. Wang, T. Wijeratne, A.S. Winkler, C.D.A. Wolfe, M. Woodward, J. H. Wu, S. Wulf Hanson, X. Xu, L. Yadav, A. Yadollahpour, S.H. Yahyazadeh Jabbari, K. Yamagishi, H. Yatsuya, N. Yonemoto, C. Yu, I. Yunusa, M.S. Zaman, S. Bin Zaman, M. Zamanian, R. Zand, A. Zandifar, M.S. Zastrozhin, A. Zastrozhina, Y. Zhang, Z.-J. Zhang, C. Zhong, Y.M.H. Zuniga, C.J.L. Murray, Global, regional, and national burden of stroke and its risk factors, 1990–2019: a systematic analysis for the Global Burden of Disease Study 2019, Lancet Neurol. 20 (2021) 795–820, https://doi.org/10.1016/S1474-4422(21)00252-0.

[7] W.J. Powers, A.A. Rabinstein, T. Ackerson, O.M. Adeoye, N.C. Bambakidis, K. Becker, J. Biller, M. Brown, B.M. Demaerschalk, B. Hoh, E.C. Jauch, C. S. Kidwell, T.M. Leslie-Mazwi, B. Ovbiagele, P.A. Scott, K.N. Sheth, A. M. Southerland, D.V. Summers, D.L. Tirschwell, Guidelines for the early management of patients with acute ischemic stroke: a guideline for healthcare professionals from the American heart association/American stroke association, Stroke 49 (2018) (2018), https://doi.org/10.1161/STR.0000000000000158.

[8] H.G. Zhao, W. Bin Li, Q.J. Li, X.L. Chen, H.Q. Liu, R.F. Feng, J. Ai, Limb ischemic preconditioning attenuates apoptosis of pyramidal neurons in the CA1 hippocampus induced by cerebral ischemia-reperfusion in rats, Sheng Li Xue Bao 56 (2004) 407–412.

[9] D.C. Hess, M.N. Hoda, M.B. Khan, Humoral mediators of remote ischemic conditioning: important role of eNOS/NO/nitrite, in: Acta Neurochir, 2016, pp. 45–48, https://doi.org/10.1007/978-3-319-18497-5_8. Suppl.

[10] J. Yang, F. Shakil, S. Cho, Peripheral mechanisms of remote ischemic conditioning, Cond. Med. 2 (2019) 61–68. http://www.ncbi.nlm.nih.gov/pubmed/32313875.

[11] K.D. Hougaard, N. Hjort, D. Zeidler, L. Sørensen, A. Nørgaard, R.B. Thomsen, K. Jonsdottir, K. Mouridsen, T.M. Hansen, T.H. Cho, T.T. Nielsen, H.E. Bøtker, L. Østergaard, G. Andersen, Remote ischemic perconditioning in thrombolysed stroke patients: randomized study of activating endogenous neuroprotection - design and MRI measurements, Int. J. Stroke 8 (2013) 141–146, https://doi.org/10.1111/j.1747-4949.2012.00786.x.

[12] K.D. Hougaard, N. Hjort, D. Zeidler, L. Sørensen, A. Nørgaard, T.M. Hansen, P. Von Weitzel-Mudersbach, C.Z. Simonsen, D. Damgaard, H. Gottrup, K. Svendsen, P. V. Rasmussen, L.R. Ribe, I.K. Mikkelsen, K. Nagenthiraja, T.H. Cho, A. N. Redington, H.E. Bøtker, L. Østergaard, K. Mouridsen, G. Andersen, Remote ischemic perconditioning as an adjunct therapy to thrombolysis in patients with acute ischemic stroke: a randomized trial, Stroke 45 (2014) 159–167, https://doi.org/10.1161/STROKEAHA.113.001346.

[13] W. Zhao, R. Che, S. Li, C. Ren, C. Li, C. Wu, H. Lu, J. Chen, J. Duan, R. Meng, X. Ji, Remote ischemic conditioning for acute stroke patients treated with thrombectomy, Ann. Clin. Transl. Neurol. 5 (2018) 850–856, https://doi.org/10.1002/acn3.588.

[14] T.J. England, A. Hedstrom, S. O'Sullivan, R. Donnelly, D.A. Barrett, S. Sarmad, N. Sprigg, P.M. Bath, RECAST (remote ischemic conditioning after stroke trial), Stroke 48 (2017) 1412–1415, https://doi.org/10.1161/STROKEAHA.116.016429.

[15] T.J. England, A. Hedstrom, S.E. O'Sullivan, L. Woodhouse, B. Jackson, N. Sprigg, P. M. Bath, Remote ischemic conditioning after stroke trial 2: a phase IIb randomized controlled trial in hyperacute stroke, J. Am. Heart Assoc. 8 (2019), https://doi.org/10.1161/JAHA.119.013572.

[16] N.M. Grilo, M. João Correia, J.P. Miranda, M. Cipriano, J. Serpa, M. Matilde Marques, E.C. Monteiro, A.M.M. Antunes, L.N. Diogo, S.A. Pereira, Unmasking efavirenz neurotoxicity: time matters to the underlying mechanisms, Eur. J. Pharmaceut. Sci. 105 (2017) 47–54, https://doi.org/10.1016/j.ejps.2017.05.010.

[17] J.R. Wiśniewski, A. Zougman, N. Nagaraj, M. Mann, Universal sample preparation method for proteome analysis, Nat. Methods 6 (2009) 359–362, https://doi.org/10.1038/nmeth.1322.

[18] A.S. Carvalho, H. Ribeiro, P. Voabil, D. Penque, O.N. Jensen, H. Molina, R. Matthiesen, Global mass spectrometry and transcriptomics array based drug profiling provides novel insight into glucosamine induced endoplasmic reticulum stress, Mol. Cell. Proteomics 13 (2014) 3294–3307, https://doi.org/10.1074/mcp.M113.034363.

[19] R. Matthiesen, G. Prieto, A. Amorim, K. Aloria, A. Fullaondo, A.S. Carvalho, J. M. Arizmendi, SIR: deterministic protein inference from peptides assigned to MS data, J. Proteonomics 75 (2012) 4176–4183, https://doi.org/10.1016/j.jprot.2012.05.010.

[20] D.W. Huang, B.T. Sherman, R.A. Lempicki, Systematic and integrative analysis of large gene lists using DAVID bioinformatics resources, Nat. Protoc. 4 (2009), https://doi.org/10.1038/nprot.2008.211.

[21] D.W. Huang, B.T. Sherman, R.A. Lempicki, Bioinformatics enrichment tools: paths toward the comprehensive functional analysis of large gene lists, Nucleic Acids Res. 37 (2009) 1–13, https://doi.org/10.1093/nar/gkn923.

[22] Z. Lu, K.B. Cohen, L. Hunter, GeneRIF quality assurance as summary revision, Pac. Symp. Biocomput. (2007) 269–280, https://doi.org/10.1142/9789812772435_0026.

[23] M. Ashburner, C.A. Ball, J.A. Blake, D. Botstein, H. Butler, J.M. Cherry, A.P. Davis, K. Dolinski, S.S. Dwight, J.T. Eppig, M.A. Harris, D.P. Hill, L. Issel-Tarver, A. Kasarskis, S. Lewis, J.C. Matese, J.E. Richardson, M. Ringwald, G.M. Rubin, G. Sherlock, Gene Ontology: tool for the unification of biology, Nat. Genet. 25 (2000) 25–29, https://doi.org/10.1038/75556.

[24] S. Carbon, E. Douglass, B.M. Good, D.R. Unni, N.L. Harris, C.J. Mungall, S. Basu, R. L. Chisholm, R.J. Dodson, E. Hartline, P. Fey, P.D. Thomas, L.-P. Albou, D. Ebert, M.J. Kesling, H. Mi, A. Muruganujan, X. Huang, T. Mushayahama, S.A. LaBonte, D. A. Siegele, G. Antonazzo, H. Attrill, N.H. Brown, P. Garapati, S.J. Marygold,

V. Trovisco, G. dos Santos, K. Falls, C. Tabone, P. Zhou, J.L. Goodman, V. B. Strelets, J. Thurmond, P. Garmiri, R. Ishtiaq, M. Rodríguez-López, M.L. Acencio, M. Kuiper, A. Lægreid, C. Logie, R.C. Lovering, B. Kramarz, S.C.C. Saverimuttu, S. M. Pinheiro, H. Gunn, R. Su, K.E. Thurlow, M. Chibucos, M. Giglio, S. Nadendla, J. Munro, R. Jackson, M.J. Duesbury, N. Del-Toro, B.H.M. Meldal, K. Paneerselvam, L. Perfetto, P. Porras, S. Orchard, A. Shrivastava, H.-Y. Chang, R. D. Finn, A.L. Mitchell, N.D. Rawlings, L. Richardson, A. Sangrador-Vegas, J. A. Blake, K.R. Christie, M.E. Dolan, H.J. Drabkin, D.P. Hill, L. Ni, D.M. Sitnikov, M. A. Harris, S.G. Oliver, K. Rutherford, V. Wood, J. Hayles, J. Bähler, E.R. Bolton, J. L. De Pons, M.R. Dwinell, G.T. Hayman, M.L. Kaldunski, A.E. Kwitek, S.J. F. Laulederkind, C. Plasterer, M.A. Tutaj, M. Vedi, S.-J. Wang, P. D'Eustachio, L. Matthews, J.P. Balhoff, S.A. Aleksander, M.J. Alexander, J.M. Cherry, S.R. Engel, F. Gondwe, K. Karra, S.R. Miyasato, R.S. Nash, M. Simison, M.S. Skrzypek, S. Weng, E.D. Wong, M. Feuermann, P. Gaudet, A. Morgat, E. Bakker, T.Z. Berardini, L. Reiser, S. Subramaniam, E. Huala, C.N. Arighi, A. Auchincloss, K. Axelsen, G. Argoud-Puy, A. Bateman, M.-C. Blatter, E. Boutet, E. Bowler, L. Breuza, A. Bridge, R. Britto, H. Bye-A-Jee, C.C. Casas, E. Coudert, P. Denny, A. Estreicher, M.L. Famiglietti, G. Georghiou, A. Gos, N. Gruaz-Gumowski, E. Hatton-Ellis, C. Hulo, A. Ignatchenko, F. Jungo, K. Laiho, P. Le Mercier, D. Lieberherr, A. Lock, Y. Lussi, A. MacDougall, M. Magrane, M.J. Martin, P. Masson, D.A. Natale, N. Hyka-Nouspikel, S. Orchard, I. Pedruzzi, L. Pourcel, S. Poux, S. Pundir, C. Rivoire, E. Speretta, S. Sundaram, N. Tyagi, K. Warner, R. Zaru, C.H. Wu, A. D. Diehl, J.N. Chan, C. Grove, R.Y.N. Lee, H.-M. Muller, D. Raciti, K. Van Auken, P. W. Sternberg, M. Berriman, M. Paulini, K. Howe, S. Gao, A. Wright, L. Stein, D. G. Howe, S. Toro, M. Westerfield, P. Jaiswal, L. Cooper, J. Elser, The Gene Ontology resource: enriching a GOld mine, Nucleic Acids Res. 49 (2021) D325–D334, https://doi.org/10.1093/nar/gkaa1113.

[25] M. Fujimura, F. Usuki, Methylmercury induces oxidative stress and subsequent neural hyperactivity leading to cell death through the p38 MAPK-CREB pathway in differentiated SH-SY5Y cells, Neurotoxicology 67 (2018) 226–233, https://doi.org/10.1016/j.neuro.2018.06.008.

[26] D. Dias-Pedroso, J.S. Ramalho, V.A. Sardão, J.G. Jones, C.C. Romão, P.J. Oliveira, H.L.A. Vieira, Carbon monoxide-neuroglobin Axis targeting metabolism against inflammation in BV-2 microglial cells, Mol. Neurobiol. 59 (2022) 916–931, https://doi.org/10.1007/s12035-021-02630-4.

[27] M.P. Murphy, H. Bayir, V. Belousov, C.J. Chang, K.J.A. Davies, M.J. Davies, T. P. Dick, T. Finkel, H.J. Forman, Y. Janssen-Heininger, D. Gems, V.E. Kagan, B. Kalyanaraman, N.-G. Larsson, G.L. Milne, T. Nyström, H.E. Poulsen, R. Radi, H. Van Remmen, P.T. Schumacker, P.J. Thornalley, S. Toyokuni, C.C. Winterbourn, H. Yin, B. Halliwell, Guidelines for measuring reactive oxygen species and oxidative damage in cells and in vivo, Nat. Metab. 4 (2022) 651–662, https://doi.org/10.1038/s42255-022-00591-z.

[28] B.B. Weksler, E.A. Subileau, N. Perrière, P. Charneau, K. Holloway, M. Leveque, H. Tricoire-Leignel, A. Nicotra, S. Bourdoulous, P. Turowski, D.K. Male, F. Roux, J. Greenwood, I.A. Romero, P.O. Couraud, Blood-brain barrier-specific properties of a human adult brain endothelial cell line, Faseb. J. 19 (2005) 1872–1874, https://doi.org/10.1096/fj.04-3458fje.

[29] C.S.F. Queiroga, A. Vercelli, H.L.A. Vieira, Carbon monoxide and the CNS: challenges and achievements, Br. J. Pharmacol. 172 (2015) 1533–1545, https://doi.org/10.1111/bph.12729.

[30] B.S. Boland, M.H. Dong, R. Bettencourt, E. Barrett-Connor, R. Loomba, Association of serum bilirubin with aging and mortality, J. Clin. Exp. Hepatol. 4 (2014) 1–7, https://doi.org/10.1016/j.jceh.2014.01.003.

[31] I. Andreadou, E.K. Iliodromitis, T. Rassaf, R. Schulz, A. Papapetropoulos, P. Ferdinandy, The role of gasotransmitters NO, H_2S and CO in myocardial ischaemia/reperfusion injury and cardioprotection by preconditioning, postconditioning and remote conditioning, Br. J. Pharmacol. 172 (2015), https://doi.org/10.1111/bph.12811.

[32] S.B.A. Cau, F.S. Carneiro, R.C. Tostes, Differential modulation of nitric oxide synthases in aging: therapeutic opportunities, Front. Physiol. 3 (2012), https://doi.org/10.3389/fphys.2012.00218.

[33] C. Trumpff, J. Michelson, C.J. Lagranha, V. Taleon, K.R. Karan, G. Sturm, D. Lindqvist, J. Fernström, D. Moser, B.A. Kaufman, M. Picard, Stress and circulating cell-free mitochondrial DNA: a systematic review of human studies, physiological considerations, and technical recommendations, Mitochondrion 59 (2021) 225–245, https://doi.org/10.1016/j.mito.2021.04.002.

[34] D. Giustarini, I. Dalle-Donne, A. Milzani, R. Rossi, Oxidative stress induces a reversible flux of cysteine from tissues to blood in vivo in the rat, FEBS J. 276 (2009) 4946–4958, https://doi.org/10.1111/j.1742-4658.2009.07197.x.

[35] R. Rossi, D. Giustarini, A. Milzani, I. Dalle-Donne, Cysteinylation and homocysteinylation of plasma protein thiols during ageing of healthy human beings, J. Cell Mol. Med. 13 (2009) 3131–3140, https://doi.org/10.1111/j.1582-4934.2008.00417.x.

[36] R. Motterlini, R. Foresti, Biological signaling by carbon monoxide and carbon monoxide-releasing molecules, Am. J. Physiol. Physiol. 312 (2017) C302–C313, https://doi.org/10.1152/ajpcell.00360.2016.

[37] C.L. Grek, J. Zhang, Y. Manevich, D.M. Townsend, K.D. Tew, Causes and consequences of cysteine S-glutathionylation, J. Biol. Chem. 288 (2013) 26497–26504, https://doi.org/10.1074/jbc.R113.461368.

[38] A. Paolicchi, S. Dominici, L. Pieri, E. Maellaro, A. Pompella, Glutathione catabolism as a signaling mechanism, Biochem. Pharmacol. 64 (2002) 1027–1035, https://doi.org/10.1016/S0006-2952(02)01173-5.

[39] E. Merck, C. Gaillard, M. Scuiller, P. Scapini, M.A. Cassatella, G. Trinchieri, E.E. M. Bates, Ligation of the FcRγ chain-associated human osteoclast-associated receptor enhances the proinflammatory responses of human monocytes and neutrophils, J. Immunol. 176 (2006) 3149–3156, https://doi.org/10.4049/jimmunol.176.5.3149.

[40] E. Merck, B. de Saint-Vis, M. Scuiller, C. Gaillard, C. Caux, G. Trinchieri, E.E. M. Bates, Fc receptor gamma-chain activation via hOSCAR induces survival and maturation of dendritic cells and modulates Toll-like receptor responses, Blood 105 (2005) 3623–3632, https://doi.org/10.1182/blood-2004-07-2809.

[41] C. Goettsch, M. Rauner, K. Sinningen, S. Helas, N. Al-Fakhri, K. Nemeth, C. Hamann, S. Kopprasch, E. Aikawa, S.R. Bornstein, M. Schoppet, L.C. Hofbauer, The Osteoclast-Associated Receptor (OSCAR) is a novel receptor regulated by oxidized low-density lipoprotein in human endothelial cells, Endocrinology 152 (2011) 4915–4926, https://doi.org/10.1210/en.2011-1282.

[42] C. Ekman, A. Gottsäter, B. Lindblad, B. Dahlbäck, Plasma concentrations of Gas6 and soluble Axl correlate with disease and predict mortality in patients with critical limb ischemia, Clin. Biochem. 43 (2010) 873–876, https://doi.org/10.1016/j.clinbiochem.2010.04.006.

[43] C. Zhu, Y. Wei, X. Wei, AXL receptor tyrosine kinase as a promising anti-cancer approach: functions, molecular mechanisms and clinical applications, Mol. Cancer 18 (2019) 153, https://doi.org/10.1186/s12943-019-1090-3.

[44] R. Di Stasi, L. De Rosa, L.D. D'Andrea, Therapeutic aspects of the Axl/Gas6 molecular system, Drug Discov. Today 25 (2020) 2130–2148, https://doi.org/10.1016/j.drudis.2020.09.022.

[45] U. Malik, A. Javed, LRIGs: a prognostically significant family with emerging therapeutic competence against cancers, Curr. Cancer Drug Targets 17 (2016) 3–16, https://doi.org/10.2174/1568009617011612022004 45.

[46] F. Cheng, P. Zhang, Q. Xiao, Y. Li, M. Dong, H. Wang, D. Kuang, Y. He, Q. Duan, F. Mao, B. Wang, D. Guo, The prognostic and therapeutic potential of LRIG3 and soluble LRIG3 in glioblastoma, Front. Oncol. 9 (2019), https://doi.org/10.3389/fonc.2019.00447.

[47] D. Lindquist, S. Kvarnbrink, R. Henriksson, H. Hedman, LRIG and cancer prognosis, Acta Oncol. (Madr.) 53 (2014) 1135–1142, https://doi.org/10.3109/0284186X.2014.953258.

[48] Y. Zhao, Z. Zou, D. Sun, Y. Li, S.C. Sinha, L. Yu, L. Bennett, B. Levine, GLIPR2 is a negative regulator of autophagy and the BECN1-ATG14-containing phosphatidylinositol 3-kinase complex, Autophagy 17 (2021) 2891–2904, https://doi.org/10.1080/15548627.2020.1847798.

[49] Z. Zhao, X. Yang, Inhibition of SMYD2 attenuates paraquat-induced pulmonary fibrosis by inhibiting the epithelial-mesenchymal transition through the GLIPR2/ERK/p38 axis, Pestic. Biochem. Physiol. 202 (2024) 105971, https://doi.org/10.1016/j.pestbp.2024.105971.

[50] S.-B. Yu, Q. Gao, W.-W. Lin, M.-Q. Kang, Proteomic analysis indicates the importance of TPM3 in esophageal squamous cell carcinoma invasion and metastasis, Mol. Med. Rep. 15 (2017) 1236–1242, https://doi.org/10.3892/mmr.2017.6145.

[51] H.-Y. Tang, L.A. Beer, J.L. Tanyi, R. Zhang, Q. Liu, D.W. Speicher, Protein isoform-specific validation defines multiple chloride intracellular channel and tropomyosin isoforms as serological biomarkers of ovarian cancer, J. Proteonomics 89 (2013) 165–178, https://doi.org/10.1016/j.jprot.2013.06.016.

[52] K. Huang, W. Yang, M. Shi, S. Wang, Y. Li, Z. Xu, The role of TPM3 in protecting cardiomyocyte from hypoxia-induced injury via cytoskeleton stabilization, Int. J. Mol. Sci. 25 (2024) 6797, https://doi.org/10.3390/ijms25126797.

[53] C.J. Valvona, H.L. Fillmore, P.B. Nunn, G.J. Pilkington, The regulation and function of lactate dehydrogenase A: therapeutic potential in brain tumor, Brain Pathol. 26 (2016) 3–17, https://doi.org/10.1111/bpa.12299.

[54] M.R. Woodford, V.Z. Chen, S.J. Backe, G. Bratslavsky, M. Mollapour, Structural and functional regulation of lactate dehydrogenase-A in cancer, Future Med. Chem. 12 (2020) 439–455, https://doi.org/10.4155/fmc-2019-0287.

[55] S.-F. Chen, M.-X. Pan, J.-C. Tang, J. Cheng, D. Zhao, Y. Zhang, H.-B. Liao, R. Liu, Y. Zhuang, Z.-F. Zhang, J. Chen, R.-X. Lei, S.-F. Li, H.-T. Li, Z.-F. Wang, Q. Wan, Arginine is neuroprotective through suppressing HIF-1α/LDHA-mediated inflammatory response after cerebral ischemia/reperfusion injury, Mol. Brain 13 (2020) 63, https://doi.org/10.1186/s13041-020-00601-9.

[56] Y. Xu, D. Xia, K. Huang, M. Liang, Hypoxia-induced P4HA1 overexpression promotes post-ischemic angiogenesis by enhancing endothelial glycolysis through downregulating FBP1, J. Transl. Med. 22 (2024) 74, https://doi.org/10.1186/s12967-024-04872-x.

[57] J. Hu, J. Wang, C. Li, Y. Shang, Fructose-1,6-bisphosphatase aggravates oxidative stress-induced apoptosis in asthma by suppressing the Nrf2 pathway, J. Cell Mol. Med. 25 (2021) 5001–5014, https://doi.org/10.1111/jcmm.16439.

[58] T. Waerner, M. Alacakaptan, I. Tamir, R. Oberauer, A. Gal, T. Brabletz, M. Schreiber, M. Jechlinger, H. Beug, ILEI: a cytokine essential for EMT, tumor formation, and late events in metastasis in epithelial cells, Cancer Cell 10 (2006) 227–239, https://doi.org/10.1016/j.ccr.2006.07.020.

[59] Z. Gao, C. Lu, Z. Wang, Y. Song, J. Zhu, P. Gao, J. Sun, X. Chen, M. Wang, Y. Dong, H. Xu, ILEI: a novel marker for epithelial–mesenchymal transition and poor prognosis in colorectal cancer, Histopathology 65 (2014) 527–538, https://doi.org/10.1111/his.12435.

[60] U. Schmidt, B. Uluca, I. Vokic, B. Malik, T. Kolbe, C. Lassnig, M. Holcmann, V. Moreno-Viedma, B. Robl, C. Mühlberger, D. Gotthardt, M. Sibilia, T. Rülicke, M. Müller, A. Csiszar, Inducible overexpression of a FAM3C/ILEI transgene has

pleiotropic effects with shortened life span, liver fibrosis and anemia in mice, PLoS One 18 (2023) e0286256, https://doi.org/10.1371/journal.pone.0286256.

[61] L. Otero-Ortega, E. Alonso-López, M. Pérez-Mato, F. Laso-García, M.C. Gómez-de Frutos, L. Diekhorst, M.L. García-Bermejo, E. Conde-Moreno, B. Fuentes, M.A. de Leciñana, S.B. Bravo, E. Díez-Tejedor, M. Gutiérrez-Fernández, Circulating extracellular vesicle proteins and MicroRNA profiles in subcortical and cortical-subcortical ischaemic stroke, Biomedicines 9 (2021) 786, https://doi.org/10.3390/biomedicines9070786.

[62] H.-S. Chen, Y. Cui, X.-Q. Li, X.-H. Wang, Y.-T. Ma, Y. Zhao, J. Han, C.-Q. Deng, M. Hong, Y. Bao, L.-H. Zhao, T.-G. Yan, R.-L. Zou, H. Wang, Z. Li, L.-S. Wan, L. Zhang, L.-Q. Wang, L.-Y. Guo, M.-N. Li, D.-Q. Wang, Q. Zhang, D.-W. Chang, H.-L. Zhang, J. Sun, C. Meng, Z.-H. Zhang, L.-Y. Shen, L. Ma, G.-C. Wang, R.-H. Li, L. Zhang, C. Bi, L.-Y. Wang, D.-L. Wang, S.-M. Geng, J. Shi, M. Sun, X.-F. Qiu, H.-T. Jiang, Y.-J. Zhang, J.-Y. Chen, R.-P. Wang, F.-S. Bai, J. Li, X.-H. Gong, Y. Bai, Y.-S. Li, Y.-F. Feng, C. Ha, C.-H. Jiang, J.-H. Zhai, B. Han, Y. Wang, D.-Y. Wang, K.-H. Yang, H.-Y. Yu, X.-K. Yu, H.-B. Xiao, C. Nie, Z. Jiao, J.-Y. Li, Z.-M. Meng, S.-Y. Chen, X.-H. Song, J. Xu, L. Li, X.-L. Wang, X.-J. Wang, W.-X. Zheng, W.-X. Zheng, Y.-J. Liu, M. Yu, J. Feng, Effect of remote ischemic conditioning vs usual care on neurologic function in patients with acute moderate ischemic stroke, JAMA 328 (2022) 627, https://doi.org/10.1001/jama.2022.13123.